THESIS

IMMUNE RESPONSE MODULATION USING TOLFENAMIC ACID AS AN EFFECTIVE THERAPEUTIC FOR *BURKHOLDERIA PSEUDOMALLEI* INFECTION

Submitted by

William J. Wilson

Department of Environmental and Radiological Health Sciences

In partial fulfillment of the requirements

For the degree of Master of Science

Colorado State University

Fort Collins, Colorado

Summer 2016

Master's Committee:

Advisor: William Hanneman

Richard Slayden
Marie Legare
Ronald Tjalkens

ABSTACT

IMMUNE RESPONSE MODULATION USING TOLFENAMIC ACID AS AN EFFECTIVE THERAPEUTIC FOR *BURKHOLDERIA PSEUDOMALLEI* INFECTION

Melioidosis is a tropical, often fatal, disease caused by the aerobic, Gram-negative facultative intracellular bacterium *Burkholderia pseudomallei.* Despite its growing global burden and high fatality rate, little is known about the disease. Recent studies demonstrate that Cyclooxygenase-2 (COX-2) inhibition is an effective post-exposure therapeutic to pulmonary melioidosis by inhibiting the production of Prostaglandin E2 (PGE2). However, this effective treatment was conducted using an experimental COX-2 inhibitor which is not approved for human or animal use, therefore, an alternative COX-2 inhibitor needs to be identified for further studies. Tolfenamic acid (TA) is a non-steroidal anti-inflammatory drug (NSAID) developed for COX-2 inhibition and is marketed outside of the United States for the treatment of migraines. While this drug was developed for COX-2 inhibition, it has been found to modulate other aspects of inflammation. In this study, we analyzed the effect of TA on cell survival, regulation of COX-2 and Nuclear factor- kappaB (NF-κB) protein expression as well as PGE2 production using RAW 264.7 cells infected with *B. pseudomallei*. We used this information to develop a protocol to evaluate the effectiveness of post-exposure treatment with TA as a therapeutic and compared these results to effective Ceftazidime treatments and the co-treatment of TA with a sub-therapeutic treatment of Ceftazidime in BALB/c mice. TA effectively increased cell viability *in vitro* and was able to reduce COX-2 expression and PGE2 production while also decreasing NF-κB activation during infection. Oral administration of TA to BALB/c mice infected with *B. pseudomallei* was

able to significantly increase survival outcome, however, this did not alter bacterial load or dissemination within organ tissues. The co-treatment of TA with a sub-therapeutic treatment of Ceftazidime was able to substantially increase survival outcome and clear the bacterial load within organ tissue. We demonstrate that post-exposure treatment with TA and sub-therapeutic Ceftazidime is effective to treat melioidosis in BALB/c mice. Additionally, we further elucidate the inflammatory response to *B. pseudomallei*.

ACKNOWLEDGEMENTS

I would like to first acknowledge my wife, Joyce. Through the crazy times and struggles you have continued to be there for me and support all of life's endeavors, always placing my needs before your own. I look forward to the next chapter in our lives. Next, my son, Bear. The days you helped me in the lab I will cherish forever. My only hope is that one day you will read this thesis and laugh at its simplicity as your foundational knowledge will greatly exceed that of my own.

Dr. William Hanneman, you are by far the best advisor a student could ask for. You treated me as a peer, never micro-managed, challenged my ways of thinking (although, I still think my ways are better) and supported all my wacky ideas all while not allowing me to fail. Your guidance these last two years has been insurmountable, and I will forever appreciate and value the relationship we have developed. I also want to thank the remaining members of my committee, Dr. Legare, Dr. Slayden and Dr. Tjalkens. The magnitude of support you have provided can only be surmounted by your desire to see students succeed and, more importantly, your sense of humor. Regardless of the struggles life would throw my way, I could never leave the building without a smile.

Finally, to my "battle buddies." Mary Afzali, you literally are the force that allowed me to succeed in the lab. You never allow me to accept defeat, would never let me give up, even when I wanted (or was told) too. All the success in our lab can be attributed to you and your efforts. I realize that often times you would concern yourself more with my success rather than your own, and for that I am forever grateful. You will make an amazing teacher that will effectively train and mentor future students and have lasting positive impact on the world. I am confident our friendship will

continue to grow and evolve as we continue down our individual paths. Lastly, Jason Cummings. I cannot remember a time where I looked forward to working with someone at every opportunity. Although I know it was grueling, you coached and mentored me in a field that made me incredibly uncomfortable. At all times in the BSL-3, I was confident not only in our work, but our safety too. I value the friendship we have developed and look forward to continuing that friendship as we both begin new chapters in our lives.

TABLE OF CONTENTS

LISTS OF FIGURES

CHAPTER 1: HYPOTHESIS AND AIMS

1.1 Chapter Introduction

Despite *Burkholderia pseudomallei*'s listing as a Tier 1 select agent by the U.S. Department of Health and Human Services (DHHS) [1] as well as naturally occurring environmental bacteria in Asia and Australia, little is known about how the disease causes mortality. Current antibiotic treatments are intense and demonstrate limited efficacy. Furthermore, because of the nature of the treatment, patients often fail to finish the prescribed course. This leads to disease relapse and a subsequent high mortality rate results among infected individuals [2]. In order to develop more comprehensive prevention strategies, it is important to better understand the course of infection and the complexity of the host response.

The human immune response is thought to be a large contributing factor to the lethality of infection [2]; however, this has not been well vetted. How does this disease activate the immune response? Which organs play a primary role in fighting the infection? Does the inflammatory response play a key role in lethality? These questions and uncertainties help formulate the hypothesis of this thesis that ***B. pseudomallei*** **alters the inflammatory response primarily through the Nuclear Factor kappa-light-chain-enhancer of activated B cells (NF-κB) pathway. Thus, modulation of this pathway early in infection will result in an increased survival in BALB/c mice.**

It has been shown that the inhibition of Cyclooxygenase-2 (COX-2) using NS-398, a non-steroidal anti-inflammatory drug (NSAID) leads to increased survival in the BALB/c model [2]. In this work I expect to better understand and describe the inflammatory pathway *in-vitro* and *in-*

vivo using a BALB/c mouse model. In order to address this hypothesis, this project is divided into two aims.

1.2 Aim 1

In order to better understand how *B. pseudomallei* affects macrophages during infection, an *in-vitro* model is needed. This model will utilize the RAW 264.7 immortalized murine macrophage-like cell line to better understand *B. pseudomallei* infection. **Aim 1 is to characterize the inflammatory response in a macrophage-like cell line in order to determine how treatment with NSAIDs may be more effective**. The main goals of this aim are to 1) determine how Tolfenamic Acid (TA) treatment of cells infected with *B. pseudomallei* with affects cell viability; and 2) determine what dose of TA is optimal for *in-vitro* treatment and compare this to other proven effective treatment strategies. NF-κB activation, COX-2 induction, and Prostaglandin E2 (PGE2) production will be analyzed as appropriate endpoints to this study.

1.3 Aim 2

The BALB/C mouse is an effective model for this research due to its commercial availability and its vast history as being utilized as a model organism for infection. **Aim 2 is to track the bacterial load of a *B. pseudomallei* intranasal infection in Balb/c mice in order to determine how treatment alters dissemination. Additionally, get a glimpse of the terminal inflammatory pathway activation.** The main aspects we will monitor are the bacterial loads of the lung, liver and spleen at 60 hours post-infection and the magnitude of the inflammatory response as measured in the peripheral blood monoclonal cells (PBMCs).

Additionally, because immune system modulation could provide a valuable treatment regime for *B. pseudomallei* infections, **Aim 2 also includes monitoring how modulating the immune response using COX-2 inhibitors translates to increased survival outcome.** COX-2 inhibitors will be compared to known effective antibiotic treatments in this model to further elucidate the immune response during infection and treatment. The aspect important in this aim are how the various treatments affect survival outcome. These results could provide valuable insight into future treatments of the disease and disease prevention.

1.4 Overview of Results

Aim 1 revealed that TA is effective at increasing RAW 264.7 cell viability during a *B. pseudomallei* level 2 surrogate (Bp82) infection and that TA reduces COX-2 and NF-κB expression *in-vitro* as well as reduces the production of PGE2. Data from Aim 2 showed that, while TA does not significantly reduce bacterial burden in the liver or spleen, it does significantly increase survival outcome. However, the co-treatment with TA and a sub-therapeutic dose of Ceftazidime also did not affect the bacterial burden at 60 hours, but substantially increased survival outcome. Furthermore, at 37 days post-infection the mice were almost completely cleared of organ bacterial burden. Thus, addition of TA into the therapeutic treatment regimen was shown to significantly enhance current antibacterial treatments of Melioidosis.

1.5 Thesis Organization

This thesis is divided into 8 chapters. Chapter 2 is a background outlining the important topics related to this research on *B. pseudomallei*, inflammation, immune modulation, and the *in-vitro* and *in-vivo* models. Chapter 3 explains the general methods used in each aim. Chapter 4 and 5 present all of the specific methodology and results of each aim individually. Chapter 6 discusses possible future research based on results obtained and Chapter 7 concludes all relevant work. Chapter 8 lists my original contributions to the field.

CHAPTER 2: BACKGROUND

2.1 Melioidosis

Melioidosis is a tropical, often fatal, disease caused by the aerobic, Gram-negative facultative intracellular bacterium *Burkholderia pseudomallei* [3]. *B. pseudomallei* is most common in Southeast Asia and Northern Australia were it is found naturally as a soil-dwelling bacteria. Melioidosis is also common in Northeastern Thailand as it accounts for 20% of all community-acquired septicemias and 40% of sepsis related mortality with an overall primary disease mortality rate of 50% [4]. Increasingly, cases of melioidosis have been reported in more diverse locations across the globe resulting in 169,000 predicted incidences a year, causing 89,000 deaths across at least 34 countries. [5] [6].

Traditional *B. pseudomallei* infection is associated with environmental/occupational exposures during the monsoon season in the tropics as this is typically when farmers begin to plant their rice crop. The primary exposure pathway is generally inhalational followed by cutaneous inoculation and ingestion [3] [7]. *B. pseudomallei* has been labeled as a Tier 1 Select Agent by the U.S. Department of Health and Human Services (DHHS) due to its ability to cause morbidity and mortality, its ease of acquisition and the simplicity of mass productions. Therefore, it has a large potential to cause a severe threat to public health and safety [1].

B. pseudomallei is naturally resistant to many antibiotics, such as penicillin, cephalosporin's and aminoglycosides, but is susceptible to antibiotics such as doxycycline, ceftazidime and chloramphenicol. Recurrence of the disease is common as a typical treatment regime lasts 20 weeks with both intravenous and oral phases of antibiotic administration. Individuals with pre-existing conditions that manifest with an altered immune response are at a

greater risk of the disease becoming fatal. Epidemiological studies have determined that the primary disease resulting in increased melioidosis mortality is diabetes [4]. This is cause for concern as the estimated worldwide prevalence of diabetes in 2013 was 382 million people with an expected prevalence of 592 million by 2035 [8]. The worldwide increase in prevalence of melioidosis is linked with the increased prevalence diabetes, anti-bacterial resistance and risk of illegitimate use as a weapon of terror. Thus an increased effort on understanding the underlying mechanism of this disease is required to subvert this worldwide increase .

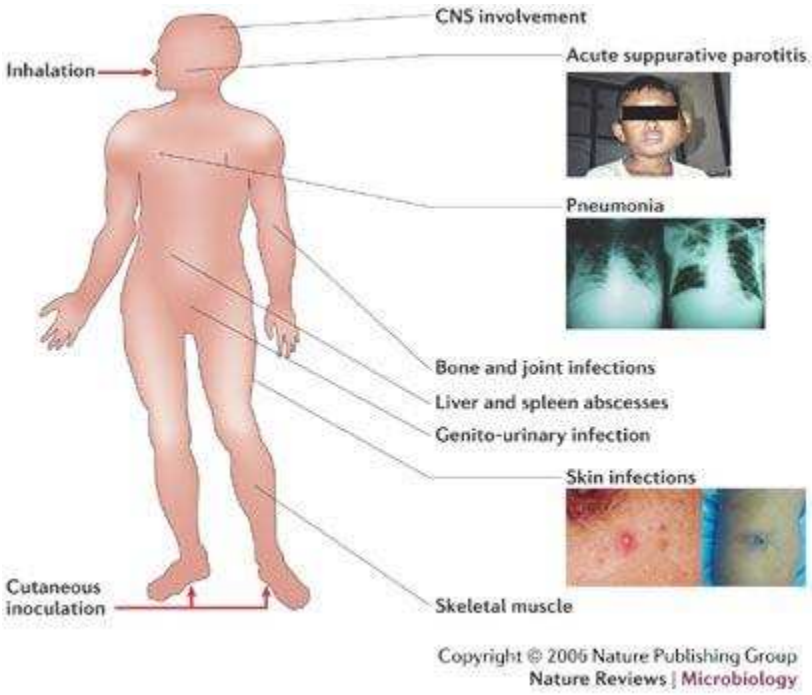

Figure 2.1. General outline of infection routes and clinical symptoms [4]. Primary routes of exposure are inhalational, ingestion and cutaneous inoculation and show a wide range of symptoms.

There are many different strains of *B. pseudomallei* [4] all with varying degrees of virulence depending on the dynamic measured. However, all strains appear to cause death in the mouse and macrophage models by similar mechanisms [3]. The progression of inhalational melioidosis is generally characterized by fast dissemination to the lungs, liver and spleen often with abscess formation in these locations. Interestingly, the geographical location of disease acquisition will affect how the bacteria is disseminated and which secondary organ systems (other than those mentioned) are effected. For instance, 33% of Thailand *B. pseudomallei*

pediatric acquired infections present with acute parotitis [4], a similar characteristic to mumps [9], whereas infections acquired in Australia can present with prostatic abscesses and brainstem encephalitis [4]. Figure 2.1 outlines the typical clinical presentations of melioidosis but are not limited to those provided. Additional clinical presentations include localized soft tissue infections and chronic localized infections in the area of inoculation [3]. In order to treat melioidosis through immune modulation, it is important to understand how *B. pseudomallei* infects the host at the cellular level and how it initiates the innate immune response.

2.2 Lifecycle and Host Response to Melioidosis

The intracellular lifecycle of *B. pseudomallei* is typical to most Gram-negative bacteria with some characteristic idiosyncrasies. *B. pseudomallei* is taken up by macrophages and leukocytes via phagocytosis. It can also invade other non-phagocytic cell types such as epithelial cells. Like most Gram-negative bacteria, it uses a type three secretion system (T3SS) called the *Burkholderia* secretion apparatus (*bsa*) in order to secrete and inject effector molecules into the host cell. Research has

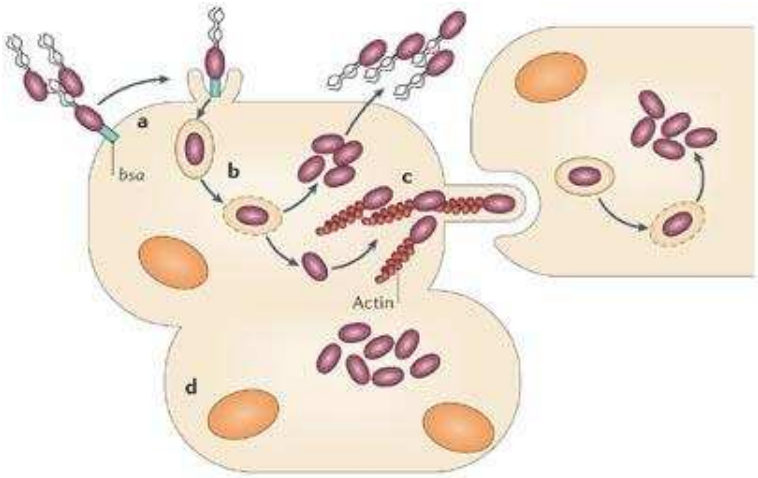

Figure 2.2. Intracellular lifecycle of B. pseudomallei [4]. Phagocytosis allows entry of the bacterium into the host cells. *B. pseudomallei* then polymerize the host actin filaments for rapid movement within the cell and into neighboring cells.

shown that the T3SS is crucial to intracellular survival, replication and virulence. Once the bacterium has entered the host cell via phagocytosis, the bacteria rapidly escapes the lysosome using the *bsa* mechanism. Studies have demonstrated that escape from the lysosome can occur in as little as 15 minutes [4] [10]. Once the bacterium enters the cytoplasm it begins to replicate. It also has a unique ability to cause polymerization of the host's cytoskeletal actin protein. Hijacking the cellular microfilament movement mechanism enables fast movement across the cell and protrusions into neighboring cells. This intracellular lifecycle is summarized in Figure 2.2.

It has been suggested that the immune response to *B. pseudomallei* infection highly contributes to its intracellular survival [2] as this bacterium has been shown to elicit an immune response through the up-regulation of pro-inflammatory cytokines in the murine model. The mechanism by which this pro-inflammatory response is initiated it not fully understood. Some research has indicated that the toll-like receptors (TLR) on the host cell surface may play an important role, while others suggest that the bacteria themselves or complement factors produced

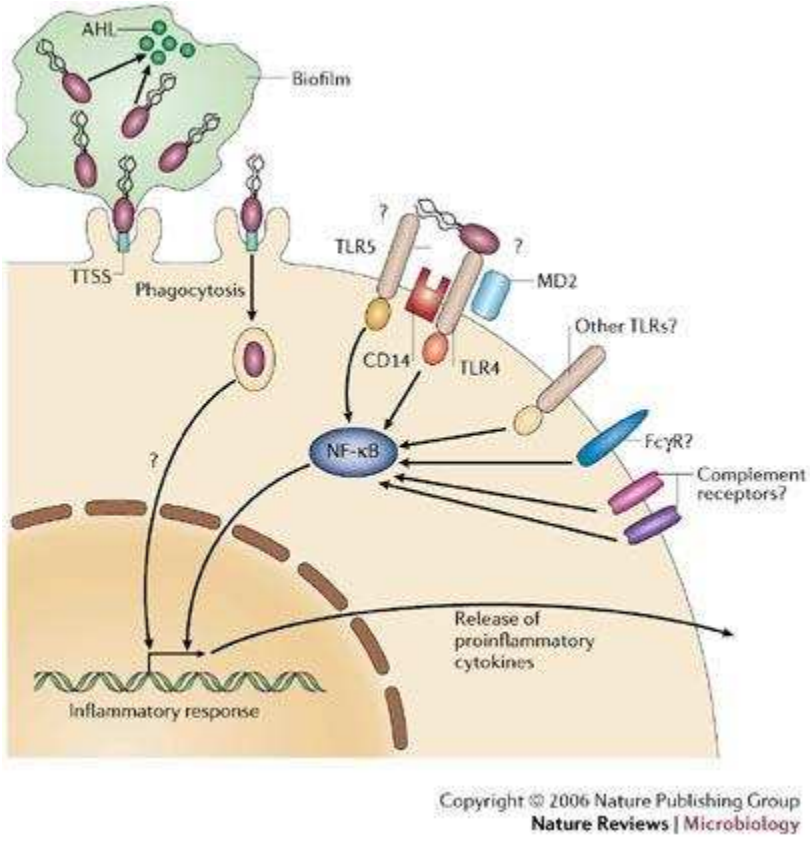

Figure 2.3. Simplified theoretical pathway of NF-κB activation during B. pseudomallei infection [4].

by the host cell may be important [2] [4]. In mice, infection with *B. pseudomallei* leads to the transcription of such pro-inflammatory markers as interferon gamma (IFN-γ), interleukins 10, 1β, 6, Keratinocyte chemoattractant (KC) and Tumor Necrosis Factor- alpha (TNF-α) [7]. All of these pro-inflammatory markers have been proven to be regulated by NF-κB [11] [12] [13] [14] [15] [16], making it an important inflammatory marker in *B. pseudomallei* infection. While there is upregulation of these cytokines, recent mechanistic studies show that infection with *B. pseudomallei* actually has a substantially lower NF-κB activation when compared to other bacteria such as *e.coli*. This is likely due to *B. pseudomallei*'s T3SS. The sequestration of the initial immune response may related to the disease's high mortality rate [17] .

More importantly, recent evidence suggests that prostaglandin E2 (PGE2) is required for intracellular survival of *B. pseudomallei* [2]. This is important as research indicates that PGE2 can work upstream of NF-κB to generate high levels of pro-inflammatory cytokines. With a positive feedback loop between PGE2 and NF-κB. Thus, the more PGE2 generated the more NF-κB is activated. This creates more pro-inflammatory cytokines to upregulate the production of PGE2 [18]. The ability of *B. pseudomallei* to survive intracellularly is key to the progression of host infection [10]. Therefore, understanding and modulating the host response are key to fighting the infection.

2.3 Immune Modulation

Research indicates that modulating a host's immune response via suppression or enhancement of key regulatory factory is an effective therapeutic strategy to combat infection. For example, hyperactivation of the immune response can often contribute to lethality in individuals with sepsis and those infected with the influenza virus. Immunomodulation, at times,

is just as effective as antimicrobial treatment with an added benefit; "it avoids the selective pressure for the evolution of microbial resistance" [19]. Because immunomodulation is nonspecific, unlike most bacterial and viral treatments, it can offer broad-spectrum protection against multiple pathogens enabling prophylactic treatment before the pathogen is known [19]. For *B. pseudomallei,* this strategy could prove to be incredibly useful in the instances of illegitimate use as bioterrorism. Although there are several targets of immunomodulation, all with unique benefits and limitations, for the purpose of this research we focus on altering the inflammatory response through the NF-κB and COX-2 pathway with the intention of limiting the production pro-inflammatory cytokines and prostaglandins, particularly PGE2.

NF-κB is a family of sequence-specific transcription factors that are present in almost every cell type and play a key role in the development and progression of inflammation [20]. As previously noted, it is responsible for the transcription of a number of cytokines that further the progression of inflammation. In its inactive form, NF-κB is bound to inhibitors of NF-κB (IκBs). When activated, the cytoplasmic IκBs are phosphorylated by IκB kinases,

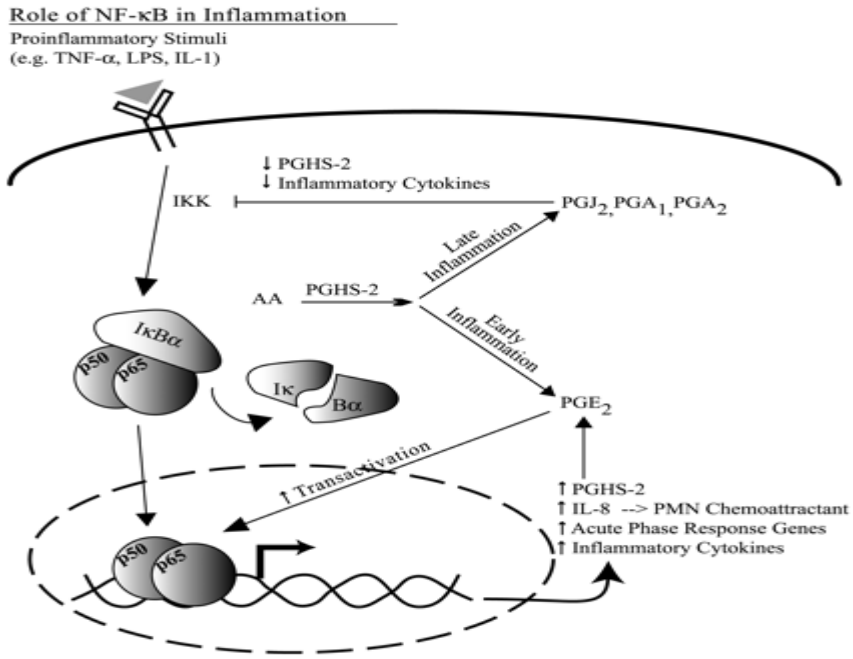

Figure 2.4. Pathway of NF-κB activation in inflammation. NF-κB activity aids in the production of PGE2 through the COX-2 pathway. PGE2 is a positive feedback allowing aiding NF-κB to cross the nuclear membrane [18].

polyubiquinated and degraded in the 26S proteosome. Once liberated the NF-κB heterodimer can migrate to the nucleus and function as a transcription factor [21]. This activation, combined with the production and secretion of cytokines, leads to the induction of COX-2, which will catalyze the conversion of arachidonic acid into several other prostaglandins. Early in infection, and of greatest importance for this research, the levels of PGE2 are high. This is troublesome in that PGE2 aids in the transactivation of NF-κB allowing for even more pro-inflammatory cytokines to be transcribed, further prolonging the duration and intensity of inflammation. This suggests a positive feedback loop between PGE2 and NF-κB. Eventually, however, PGE2 levels decrease allowing cyclopentane prostaglandin ssuch as to exert their inhibitory effects [16]. This basic pathway is illustrated in Figure 2.4.

As a counter balance to the PGE2/ NF-κB positive feedback, COX-2 expression inhibits translocation of NF-κB to the nucleus, representing a negative feedback loop [18]. Targeting COX-2 presents a therapeutic target as this may reduce the production of prostaglandin production and limits the extent of NF-κB translocation to the nucleus. Against *B. pseudomallei* the NF-κB/COX-2 relationship presents a possible prophylactic and therapeutic target but identifying whether this pathway will enhance survival via immune modulation remains to be seen. Targeting NF-κB has been effective in other bacterial infections such as *P. aeruginosa* [22].

As previously discussed, it has been shown that *B. pseudomallei* is dependent on PGE2 for intracellular survival [2]. If this is accurate, then targeting this prostaglandin pathway could prove to be an effective therapeutic target as it is limiting the only part of the entire inflammatory response which *B. pseudomallei* is dependent. Figure 2.5 demonstrates how *B. pseudomallei* (and other bacteria) influence the production of PGE2. First, Arachidonic acid (AA) is released from

the cellular membrane and COX-1 (not inducible) and COX-2 (inducible) use AA as a precursor substrate for Prostaglandin H2 (PGH2), which in then converted to PGE2 via PGE2 synthase. PGE2 then can elicit its actions on four eicosanoid receptors (EP), noted as EP1-4. Each receptor has varying affinity for PGE2 and each receptor has been shown to have various effects on the immune response. For example, EP2 and EP4 have shown to have anti-inflammatory and immunosuppressive activity when activated through a G-coupled receptors. This can result in inhibition of macrophage activation and macrophage attraction [23]. EP4, on the other hand, can also signal through a phosphatidylinositol 3-kinase (PI3K)-dependent manner which can then activate the extracellular-signal-regulated kinase 1/2 (ERK1/2) pathway. The exact mechanism and effect of each EP and PGE2 is not well understood and it appears activation and inhibition of these receptors has different outcomes in varying states of disease. However, the importance of PGE2 during inflammation is well established, hence, modulating PGE2 and other prostaglandins through the COX-2 pathway presents as a possible effective therapeutic strategy to infection.

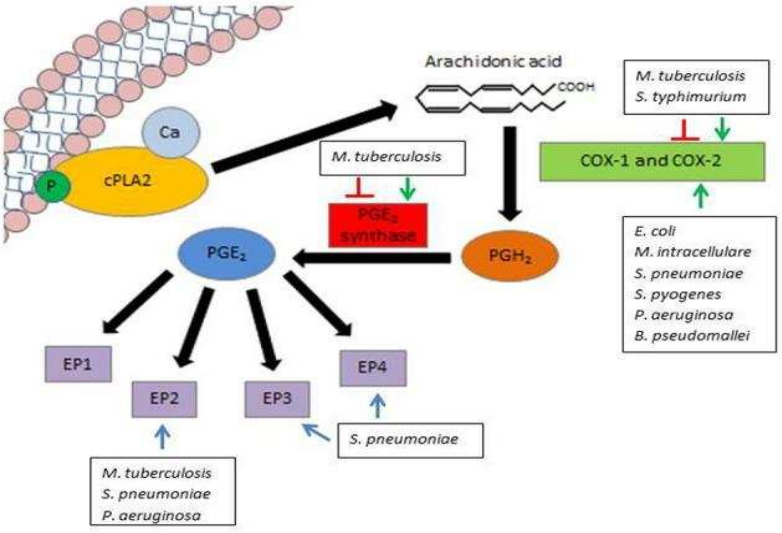

Figure 2.5. Illustration of how *B. pseudomallei* (and other pathogens) can induce COX-2 and lead to the production of PGE2. Green arrows indicate activation of COX-2 and red lines indicated inhibition [23].

2.4 Non-Steroidal Anti-inflammatory Drugs (NSAIDs)

The primary target for most NSAIDS is COX-2. COX-2 is an intracellular homodimer, however, only one monomer is used for substrate binding. It is at the substrate binding monomer site where most NSAIDs bind to inactivate the enzyme thereby halting the production of prostaglandins [24]. Accordingly, the NSAIDs in this study, Tolfenamic Acid (TA) and NS-398, have been reported to work by inactivating COX-2 through competitive inhibition at the active site [25] [26] [27]. While COX-2 inhibition prompted development of these drugs, both drugs have other characteristics that aid in controlling the immune response to pro-inflammatory stimuli.

TA belongs to the fenamate class of NSAIDS and can be administered orally, subcutaneously, intraperitoneally, or intravenously to various animal species. It is traditionally used to treat migraines with a 200mg oral dose [28]. After administration, it binds rapidity to plasma proteins (about 99.7%) and is distributed to the tissues in the body where it exerts therapeutic effects [29] [27]. It then undergoes oxidative biotransformation and is eliminated in the urine as a glucuronide conjugate [30] . TA is most widely known for its ability to selectively inhibit COX-1 and COX-2 to limit prostaglandin production; however, research spanning over 20 years also indicates that TA has therapeutic effects through many other mechanisms. A few of these other mechanisms include: inhibiting calcium influx in leukocytes to administer anti-inflammatory effects as COX-2 is calcium dependent [31] and decreasing specific protein transcription factors associated with tumor growth and metastasis in lung and colon cancer [32]. Of relevance to this research, TA has also been shown to affect NF-κB, yet, the limitation of effects and the mechanism of action on NF-κB is not well elucidated. Jeong *et al.* reported that TA has shown to activate NF-κB in human colorectal cancer cells by degrading IκBs [26], yet, that same group reported TA down-regulated NF-κB in lipopolysaccharide (LPS) stimulated

RAW264.7 macrophages [20]. Further masking the influence of TA on NF-κB, Satya and Safe (2014) recently showed that TA significantly reduced cytoplasmic concentration of activated NF-κB in colon cancer cells [33]. It would seem that the effect of TA on NF-κB depends heavily on the cell type and method of NF-κB activation, thus leaving a wide range of future studies for this compound.

NS-398 is a specific COX-2 inhibitor not currently not used clinically. However, it has shown to be exceptionally effective at limiting the production of prostaglandins [34]. This indicates that this drug has a small therapeutic window, which is not conducive to therapeutic treatment. Similar to TA, NS-398 has other targets in addition to inhibiting COX-2. Recent studies have indicated that NS-398 is an effective NF-κB activation inhibitor during inflammation as well as an effective treatment for certain types of cancer [25]. The therapeutic endpoints for this drug may prove to be an issue in human and animal use due to its high potency and likely narrow margin of safety. Hence, TA could prove to be a valuable alternative to NS-398 for *B. pseudomallei* infection treatment.

2.5 *In-Vitro* Model

The ideal cell line for this *in-vitro research* is one that has both a established response and interaction with bacterial infections and is a good model for inflammation. For this reason, the immortalized mouse macrophage-like RAW264.7 cell line was chosen. This cell line originated from a BALB/c mouse strain that was inoculated with an Abelson murine leukemia virus allowing the cell line to propagate effectively with high efficiency. As of 2008, this cell line had been chosen by the Alliance for Cellular Signaling as the primary experimental system

for cell signaling pathways. This selection is mainly due to the cells ability to produce measurable pro-inflammatory mediators and responses. Additionally, the RAW cell line is well-suited for DNA transfection and possess receptors for many relevant ligands [35]. The use of this cell line translates directly to this research as these cells will interact with *B. pseudomallei* in a manner similar to that depicted in Figure 2.2. The RAW264.7 BALB/c background allows for translation into the *in-vivo* study since the mouse model utilized will be a wild-type BALB/c mouse.

2.6 Mouse Model

In order to properly determine how the innate immune systems responds to infection and how immune modulation affects disease outcome, an *in-vivo* model is needed. Several models exist for studying melioidosis but the most prevalent model is that of wild type BALB/C mice [36]. This model is a good extension for the *in*-vitro work done in Aim 1 because RAW cells derived from a BALB/c background. Additionally, the bacterial burden in the spleen in the BALB/c mice after *B. pseudomallei* infection is high and allows us to characterize the effectiveness of treatment and dissemination of the disease [36].

2.7 Summary of Study

In this study, we analyzed the role of inflammation during pulmonary infection with *B. pseudomallei.* First, we analyzed the characteristics of the immune response and how treatment with NSAIDs effects the immune response and survival outcome in-vitro using RAW264.7 cells. This data was used to further develop our in-vivo protocol where we monitored the bacterial

dissemination and load of *B. pseudomallei* through the major organ systems to determine if there is a relationship between bacterial dissemination and treatment and how treatment affects survival outcome over time.

CHAPTER 3: MATERIALS AND METHODS

3.1 Chapter Introduction

In this chapter, the materials and methods forming the foundation of each aim is discussed. This includes general reagents, *in-vitro* cell-line maintenance and mouse handling. Specific methodology regarding treatment and data collection for each aim can be found in each respective chapter.

3.2 Reagents, NSAIDs, and Antibodies

Di-methylsulfoxide (DMSO) was purchased from ATCC (Manassas, VA). DMEM and Trypsin used for cell culture were purchased from GE Healthcare Sciences (Hyclone) (Logan, UT) and FBS+ was purchased from Atlas Biologicals (Fort Collins, CO). Tolfenamic Acid and NS-398 where purchased from Cayman Chemical (Ann Arbor, MI). Nf-κB monoclonal antibodies where purchased from Santa Cruz Biotechnology (Paso Robles, CA) and the secondary alexa fluor antibodies, 647 and HRP secondary antibodies used for all applications were purchased from Cell Signaling Technologies (Danves, MA). Luria-Bertani (LB) agar, cation adjusted Mueller-Hinton broth (ca-MHB) and COX-2 monoclonal antibodies were purchased from BD Sciences (Franklin Lakes, NJ). Dibutylhydroxytoluene (BHT), Ceftazidime, and sodium dodecyl sulfate (SDS) was purchased from Sigma-Aldrich (St. Louis, MO). Western Bright™ was purchased from Advansta (Menia Park, CA). ETDA free protease inhibitor and formalin was purchased from ThermoFisher Scientific (Waltham, MA).

3.3 In-vitro Maintenance

RAW 264.7 cells were purchased from ATCC and maintenance was performed to the company's specifications. Cells were grown in Dulbecco's Modified Eagles Medium (DMEM) with 4 mM L-glutamine, 4500 mg/L glucose, 5 mM sodium pyruvate (Hyclone), 1500 mg/L sodium bicarbonate, and 10% Fetal Bovine Serum (FBS). Cells were grown in an incubator at 37°C with 5% CO2. All cell media was replaced every 2 to 3 days or as needed based on media color change and cell confluency.

To subculture, all media was removed from the culture flask and washed with PBS (pH 7.4). The volume used for wash depended on the size of the flask and the subjective amount of noticeable debris. PBS was removed and 0.25% trypsin was added to the flask and incubated for no more than 5 minutes in order to detach the cells from the flask. Physical agitation was used to help dislodge the cells, if necessary. The trypsin was neutralized with complete DMEM and cells were subcultured in a ratio of 1:3 or 1:6 depending on experimental timeline. For each experiment, all media plus cells were removed from the flask, placed in a conical vial and centrifuged for 5 minutes at 500 rpm. The supernatant was removed and the cells were suspended in complete DMEM and counted manually using a hemocytometer. All counts were performed in duplicate and the average of the counts was used to determine the experimental cell number. All cell culture was performed in a class 2 Bio-safety cabinet.

3.4 Flow Cytometry Analysis

All flow cytometry analysis was conducted on a Beckman Coulter CyAn ADP Flow Cytometer operating Summit 4.3 software for data collection. All further data analysis was done with Flowjo software.

3.5 Western Blotting Analysis

All western blotting analysis was conducted on a Bio-Rad Chemi Doc system running Image Lab software. All further analysis was conducted on Imagej software.

3.6 Mouse Protocol

All animals were cared for in accordance with the Colorado State University Institutional Animal Care and Use Committee (IACUC) standard operating procedures. Five to Six week old BALB/c mice (Jackson Laboratories) were maintained under pathogen-free conditions and allowed free access to sterile food and water with 12 hour light/dark cycles. Anesthesia was conducted using Ketamine/xylazine (100/10 mg/kg) which was administered prior to intra-cardiac blood draw and for inoculation with *B. pseudomallei* 1026B. Euthanasia endpoints included loss of 20% body weight or more, hunched posture, reduced or absent response to stimuli, or any indication of paralysis and was conducted via cervical dislocation. All mouse studies utilizing *B. pseudomallei* 1026b were done under Animal Bio-Safety Level 3 containment.

CHAPTER 4: AIM 1

4.1 Chapter Introduction

The objective of this aim was to identify if treating macrophage-like cells *in-vitro* with TA will result in similar outcomes as previous studies with other COX-2 inhibitors. Additionally, it allowed for the mechanism of how TA increases cell survival with *B. pseudomallei* infection to be further elucidated. To accomplish these goals, a technique to measure cell survival was established as many current methods to determine cytotoxicity cannot not be used due to bacterial infection interferences. After this method was optimized, the ideal bacterial multiplicity of infection (MOI) was established. Following MOI identification the most effective treatment of TA could be established. From there, TA was compared to another effective immune modulating drug. The mechanism by which TA elicits its effects on the cell line was elucidated through determining the minimum inhibitory concentration (MIC) of the drugs, flow cytometry, western blotting, immunofluorescence and enzyme linked immunosorbent assay's (ELISA).

4.2 *Burkholderia Pseudomallei* 82

Due to *B. pseudomallei* being categorized as a select agent with a high potential for airborne transmission, all work required with this agent must be done in a bio-safety level 3 (BSL-3) laboratory. The safety protocols in these facilities often make work very difficult, expensive and unproductive to conduct even the most basic tests, therefore, *in-vitro* studies will often use surrogate organisms with little to no pathogenicity in BSL-2 facilities. This allows identifying the mechanism of disease without significant health risks and allows for monitoring

alterations in cytotoxicity, even when the bacterial surrogate is not lethal to a whole organism. This is precisely the case with Bp82.

The majority of other *B. pseudomallei in-vitro* studies are conducted with *B. thailandensis*, an organism commonly found with *B. pseudomallei* and shown to behave similar *in-vitro* [2]. However, due to the uniqueness of this disease, it was felt that an attenuated strain of the parent bacteria was needed. Propst *et al* (2010)at Colorado State University developed an avirulent strain of 1026b, named Bp82, which is incapable of adenine and thymine biosynthesis. Although Bp82 is not able to biosynthesize these nucleic acids, it is able to replicate in rich media and displays an infection mechanism in the same way as 1026b. While Bp82 is generally not lethal to a whole organism, it follows a similar lethality and immune response pattern *in-vitro* and is an effective surrogate to 1026b infection models [37]. All Bp82 stock used in this Aim was provided by Dr. Richard Slayden at Colorado State University.

4.3 Infection-Based Cytotoxicity Protocol Development

There are several methods to determine the extent of cytotoxicity induced by chemicals, however, determining cytotoxic endpoints induced by bacterial infection is much more difficult and time consuming. Quick and effective cytotoxicity methods, such as the MTT assay, or a more modern technique using the compound Almar Blue®, rely on redox reactions by living cells to produce a color change that can be measured by spectrophotometry. As *B. pseudomallei* is also a living organism, it can also perform the redox reactions that produce this color change during infection. Therefore, the aforementioned techniques would assess the viability of both the mammalian cells and *B. pseudomallei* and invalidate the assay. Another method used to assess

cytotoxicity involves manual cell counting of viable cells after fixation. This method would prove to be prohibitively time consuming as the plating densities and number of experiments run in this aim were too high. To overcome these challenges, adjustments were made to an older, yet effective, cytotoxicity technique.

The use of Crystal Violet (CV) has been used to stain mammalian cells *in-vitro* for over 28 years [38]. Originally, Christian Gram developed the Gram stain in 1883 and it is still used today as a fundamental characteristic to classify bacteria. When stained with CV, Gram-positive bacteria retain the purple color within their cell wall, even after washing due to a thick layer of peptidoglycan. Gram-negative bacteria do not retain CV when washed [39]. The fact that mammalian cells retain CV and Gram-negative bacteria, such as *B. pseudomallei*, do not retain the dye proved a useful tool to distinguish between to the two during infection.

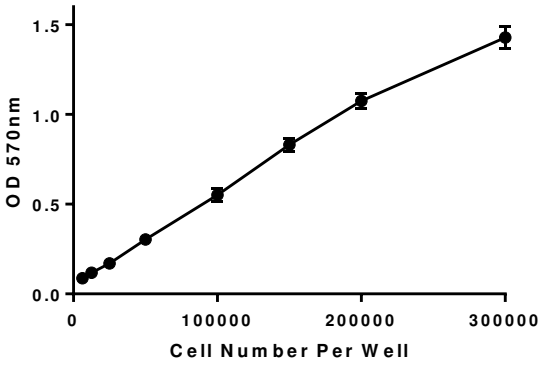

Figure 4.1. Regression analysis of 6,250-300,000 cells per well. Points show mean +/- SEM of three biological replicates each with 10 technical replicates.

The next step was to adapt the CV stain for use with Bp82. Attempting to find the most effective protocol for CV cytotoxicity staining in a 96 well plate was difficult as there are several variations of the protocol in circulation, all with different concentrations and reagents. Using a combination of two effective procedures in published literature [40] [41] along with trial and error proved successful. After optimization, RAW 264.7 cells were plated in the densities shown in Figure 4.1, allowed to incubate at 37°C with 5% CO2 for 8 hours for the cells to adhere and the procedure described in section 4.4 was executed. This resulted in a linear R^2 value of 0.993, verifying that the method is effective at

quantifying cell viability. The procedure for analyzing Bp82 induced cytotoxicity is explained in the next section.

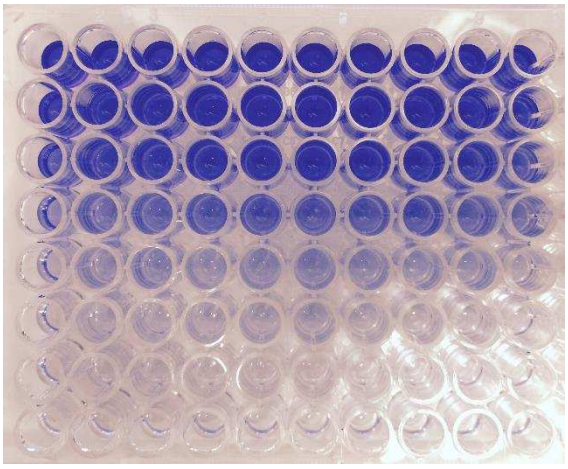

Figure 4.2. Visualization of plating densities for 300,000 cells per well (top row) to 6250 cells per well (bottom row) using the CV method. Each biological replicates had ten technical replicates**.**

4.4 Materials and Methods: Bp82 Induced Cytotoxicity

In order to properly determine what MOI was ideal for use in further experiments, a dose-response with bacterial MOI had to be investigated. To do this RAW264.7 cells were obtained from three flasks, each at different pass numbers, and prepared for experimentation as described in Chapter 3, section 1. Cells were plated in a 96-well plate at a density of 100,000 cells per well in complete DMEM. Cells were plated to account for six treatment groups each with 10 technical replicates with only 1 biological replicate. The plates were incubated at 37°C with 5% CO2 for 24 hours to allow the cells to adhere to the plate and normalize.

After 24 hours of incubation, each well was aspirated and washed two times with PBS. Each treatment group was then infected with a MOI of 0, 1, 5, 10, 25, and 50 by adding the

corresponding volume of Bp82 stock to individual vials of complete DMEM to achieve the proper MOI at 200µL. 200µL of the infected media was then added to the corresponding wells. The plates were incubated at 37°C with 5% CO2 for 2, 4, 6, 8, 10 and 12 hours.

At each time point, the media was aspirationed and the wells were washed two times with PBS. 100µL of 10% formalin in methanol was added to each treatment well and placed on a rocker for 15 minutes with 20 tilts per minute. The formalin solution was completely removed via aspiration. After the formalin was removed, 100µL of a 0.5% solution of CV in a 25% methanol, 75% ddH2O was added to each well and placed on the rocker for 15 minutes. After the dyeing process was complete, the 96 well plate was gently washed under tap water until the water ran clear from each well. The plate was either air dried overnight or placed in an isotemp oven at 40°C until dry. Finally, the CV was re-suspended by adding 100µL of 1% sodium dodecyl sulfate (SDS) solution to each well and placed on the rocker for 30 minutes at room temperature. The plate was then read on a plate reader at 570nm and 600nm. 570nm was used as the primary wavelength as described by Khursheed *et al* [40] but each absorbance was confirmed at 600nm for consistency as done by Castro-Garza *et al* [41]. This experiment was done in triplicate with each replicate having at least nine technical replicates.

To ensure that the infection was effective, percent cell viability was calculated using the uninfected control for each time point. Each sample's absorbance in each treatment group was normalized to the average absorbance of the non-infected replicates.

4.6 Results: BP82 Induced Cytotoxicity

After the 12 hour time course the data obtained is depicted in Figure 4.3. In summary, at an MOI of 50, a little over 30% cell viability was seen after 4 hours followed closely by the MOI

of 20 with 50% cell viability after 4 hours and an MOI of 10 with 65% cell viability. The MOI of 5 revealed a moderate level of cytotoxicity with little variation. The MOI of 3 revealed moderate cytotoxicity after 4 hours, where the MOI of 1 did not experience cytotoxicity until after 8 hours. These results are summarized in Figure 4.3.

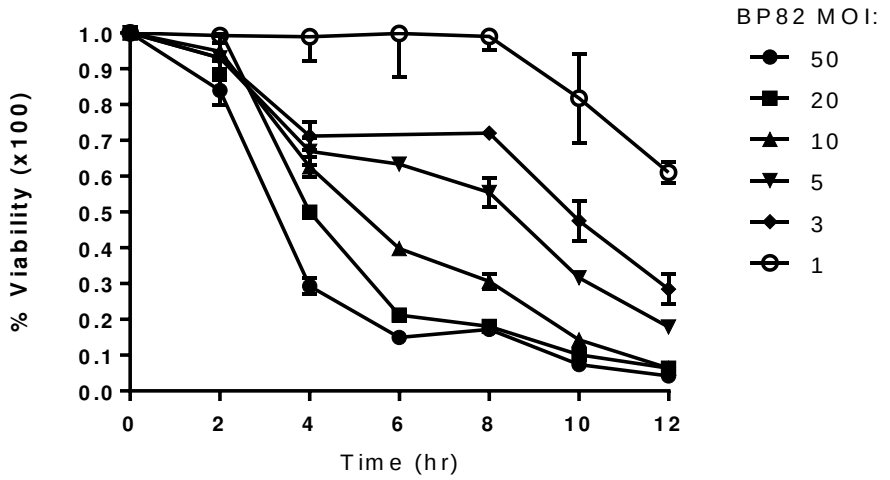

Figure 4.3. Cytotoxicity induced by different MOI's of BP82. For each time point, RAW 264.7 cells were infected with MOI's of 1, 3, 5, 10, 20 and 50 along with an uninfected control. Cytotoxicity was determined via the CV method by using the optical absorbance of each well and dividing it by the uninfected control. This experiment was done with 10 technical replicates with only one biological replicate.

4.7 Discussion: BP82 Induced Cytotoxicity

As expected, cytotoxicity induced by BP82 occurred in a dose dependent manner with the higher MOI causing the greatest amount of cytotoxicity and the lowest causing significant cytotoxicity at extended time points. The goal of this experiment was to determine both the

effective MOI of Bp82 to use in further experiments and what time points after infection appear to be ideal for elucidating the inflammatory mechanism of disease.

A MOI of 5 was selected for the ideal Bp82 for three main reasons. First, it doesn't cause significant cytotoxicity at 2 hours. This prevents overwhelming the cell culture and provides time for an appropriate cellular response to infection. Second, the MOI of 5 showed sufficient cytotoxicity after only 4 hours. This ensures an optimal window in which to measure immune response whereby cell supernatant would contain relevant levels of cytokines, prostaglandins other cell signaling molecules as these molecules often have a short half-life due to instability [42]. Lastly, the MOI of 5 reveals a stable decrease in cytotoxicity without much variation, where the other MOI's did not maintain this consistency. This experiment was only conducted one time with 10 technical replicates as it was a pilot study to determine the most effective dose of Bp82.

4.8 Materials and Methods: Effect of TA on BP82 Induced Cytotoxicity

RAW 264.7 cells were prepared for experimentation as described in Chapter 3.1. Cells were diluted and plated at a density of 100,000 cells per well in complete DMEM in a 96 well plate. Cells were plated with 10 technical replicates at time points of: 4, 6, and 8 hours after infection. Plates were incubated at 37°C with 5% CO2 for 24 hours to allow the cells to adhere to the plate and normalize.

After 24 hours, the media was apirated, washed two times with Phosphate Buffer Solution (PBS) and the appropriate treatment dilutions were added to each treatment group with 10 replicated per treatment group. Initially, these treatment groups included 200µM, 150µM, 100µM, 50µM, 20µM, 10µM, and 5µM TA along with and infected control (190µL of complete

media), non-infected control (200µL of complete media) and 0.01% DMSO in complete media as a vehicle control. After treatment, the cells were placed in the incubator for 30 minutes at which time they were infected with Bp82 with a MOI of 5, meaning that each well was infected with a total of 500,000 Bp82. This was done in 10µL per well, bringing the volume of each well to 200µL. It is important to note that the addition of the 10µL to the initial 190µL of pretreat reduced the concentration of the treatment by 5%. Therefore, cells pre-treated with 200µM TA contained 190 µM after infection. The data rreported indicates the pre-treatment concentrations.

At 4, 6, and 8 hours after infection, the media was removed and the wells were washed two times with PBS. 100µL of 10% formalin in methanol was added to each treatment well and placed on a rocker for 15 minutes with 20 tilts per minute. The formalin solution was removed by flicking the plate over the sink until there was no longer any solution visible in well. After the formalin was removed, 100µL of a 0.5% solution of CV in a 25% methanol, 75% ddH2O was added to each well and placed on the rocker for 15 minutes. After the dyeing process was complete, the 96 well plate was gently washed under tap water until the water ran clear from each well. The plate was air dried overnight or in an isotemp oven at 40°C until there was no visible liquid in any well. Finally, the CV was re-suspended by adding 100µL of 1% sodium dodecyl sulfate (SDS) solution to each well and placed on the rocker for 30 minutes at room temperature. The plate was then read on a plate reader at 570nm and 600nm. 570nm was used as the primary wavelength as described by Khursheed *et al* [40] but each absorbance was confirmed at 600nm for consistency as done by Castro-Garza *et al* [41]. This experiment was done in triplicate with each replicate having at least 9 technical replicates.

To determine percent viability, each sample's absorbance was normalized to the average absorbance of the non-infected control at the corresponding time point, providing an overall

percent viability. The percent viability was then compared to infected control without treatment using a one-way analysis of variance (ANOVA) to determine significance. After all replicates were complete, the replicates analyzed via 2-way ANOVA Bonferroni's post-hoc test was performed to determine significance and if variation occurred in the replicates. All statistical analysis was conducted using Prism 6.0 software.

4.9 Results: Effects Immune Modulation on Cytotoxicity In-vitro

Following cell viability quantification via cytotoxicity testing and identification of the infection window, the potential of immune modulation to increase cell viability during Bp82 infection could be elucidated. Figure 4.3 reveals the effects of TA on RAW 264.7 cells during Bp82 infection over time. To determine significance, all replicates were compared to the uninfected control using a 2-way ANOVA with Bonferroni's post-hoc test for significance among multiple comparisons and normalized to the uninfected control to determine percent viability.

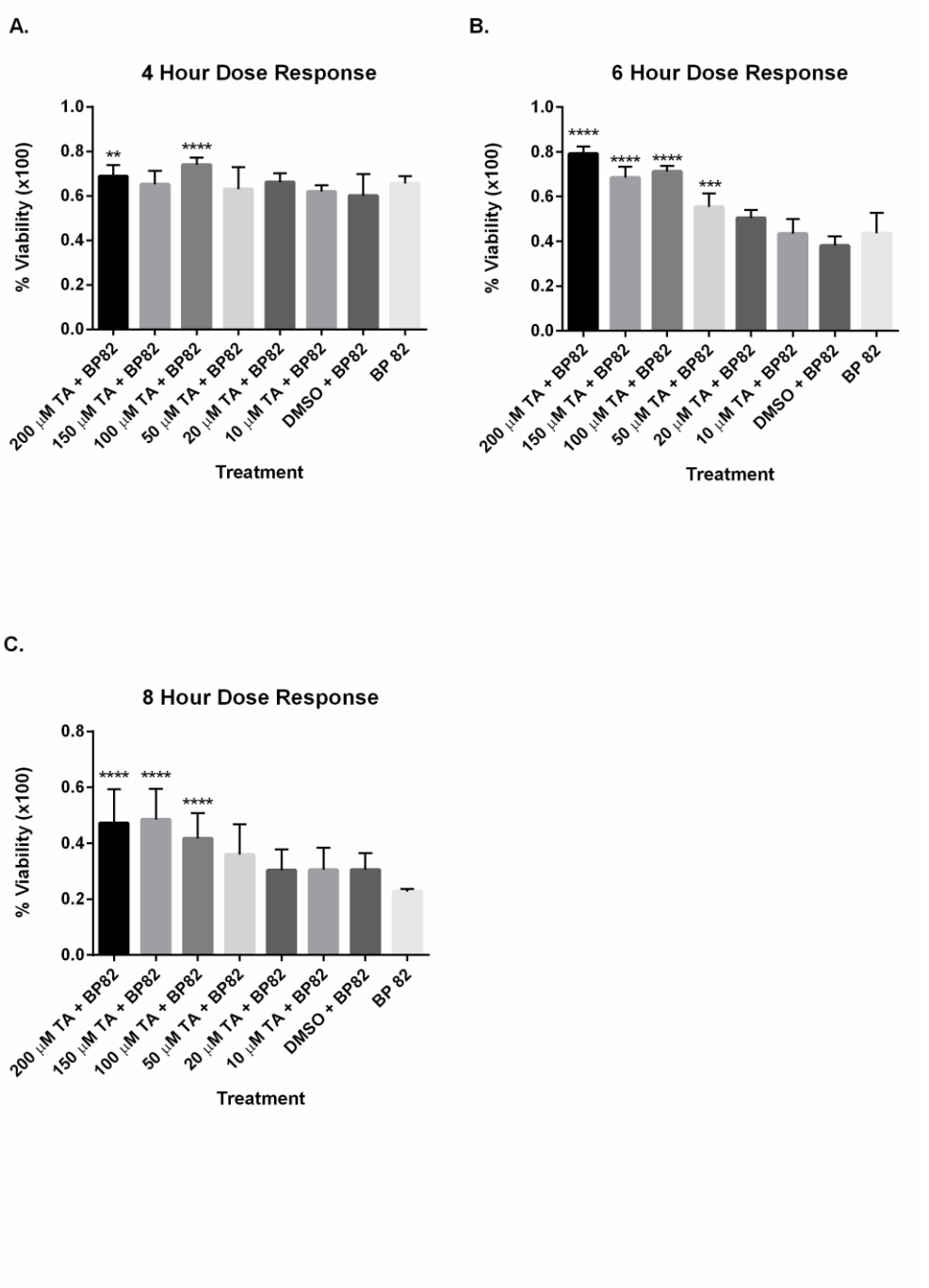

Figure 4.4. The effect of immune modulation on RAW 264.7 cell viability when infected with Bp82 over time. For each time point, cells were pretreated with the respective concentration of TA along with a 0.01% DMSO vehicle control, and had an uninfected and infected control. Optical absorbance of each technical replicate at 570nm was normalized to the average uninfected control optical absorbance and biological replicates were compared to the vehicle control (DMSO) via 2-way ANOVA with Bonferroni's test for significance. Significance was observed at all time points (A-C). *$p<0.05$, **$p<0.01$ ****$p<0.0001$.

It is clear from the data presented in Figure 4.3, that TA treatment increased cell survival at all time points post infection. This experiment was not extended past 8 hours because at this point the infected control had less than 25% cell viability and it was determined through pilot studies that extending this experiment longer would introduce greater error within the sample groups. Although both 200µM and 150 µM treatments revealed a large increase in cell viability, both of these treatment groups had large fluctuations and did not follow the traditional dose response, particularly at 4 hours where cell viability was decreased in relation to the 100 µM treatment. While there is no significance, it appears that 150µM and 200µM actually decrease cell viability initially, indicating that without infection these doses could induce cytotoxicity. Treatments from 10µM to 100µM followed the expected dose response in both 6 and 8 hours post infection with 100µM increasing cell viability in a reliable fashion by 27% and 20% at 6 and 8 hours respectively.

4.10 Discussion: Effects of Immune Modulation on Cytotoxicity In-vitro

The level of increased cell viability with the *in-vitro* treatment with TA is detailed in Figure 4.4. This follows the expectations as discussed by Asakrah *et al* (2013) [2], that a COX-2 inhibitor increases cell viability. However, here we were able to clearly shown that the cell viability is increased with TA treatment as compared to the vehicle control. Additionally, the treatment of RAW cells with TA followed a typical dose response curve until 150µM treatments. It would appear that at 8 hours, DMSO afforded some protection from cell death, whereas the other time points DMSO treatments appeared to decrease cell viability. While there is no valid explanation for this at this time point, it is worth mentioning that statistical analysis showed no

significance between the DMSO treated and untreated groups at 8 hours, even though Figure 4.3C appears to reveal that treatment with DMSO and 10µM TA result in similar cell viability.

It is interesting to note that in treatments exceeding 100µM, there is variability in cell viability over time. This is likely a result as the high concentrations of TA beginning to cause cytotoxicity. Other published research using TA *in-vitro* confirm that a 100µM concentration is the most effective. This research, however, used TA to reduce tumor size and increase anti-cancer activity in colon cancer cells [33]. Although there are drastic differences in the end-state goals in the published research by Pathi and Safe (2014) and the goals of this research, similar mechanisms were studied. For instance, 100µM treatments were shown to drastically reduce the activation NF-κB [33], which is a goal in this research; to further elucidate how TA effects the inflammatory pathways *in-vitro* during infection with Bp82. Because the 100µM treatments followed the traditional dose response expectations by increasing cell viability without any significant cell death initially as well as shown to be effective in other published work, 100µM was chosen as the ideal treatment dose for further experimentation.

4.11 Materials and Methods: Comparing NSAIDS

As the previous section explained, TA drastically increased the survival of macrophage-like cells infected with Bp82. However, it is not known how the effectiveness of TA is compared to other immune modulators such as NS-398. As indicated by previous research, NS-398 also increased the survival of macrophage-like cells *in-vitro* [2].

To compare these drugs, the procedure explained in section 4.7 was adopted. RAW cells were plated in a 96-well plates at a concentration of 100,000 cells per well and incubated for 24

hours. Three time points were chosen for these experiments: 4, 6 and 8 hours. Wells were washed two times with sterile PBS and pretreated with either 100µM TA, 100µM NS-398 or 0.01% DMSO for 30 minutes before infection with Bp82 at an MOI of 5, or media as a negative infection control. Each time point also included an untreated/infected control and an uninfected/untreated control. Each treatment had a technical replicate of 10 and the experiment was run in biological triplicate for statistical significance. Results were compared using a 2-way ANOVA with Bonferroni's post-hoc test for significance.

4.12 Results: Comparing NSAIDS

The outcome of this comparison was quite surprising. The treatment of the RAW 264.7 cells with TA reduced cytotoxicity induced by Bp82 by 8% at 4 hours, by 42% at 6 hours and 30.36% at 8 hours when compared to the DMSO treated group. By comparison, NS-398 was unable to reduce cytotoxicity at 4 hours and only reduced it by 20.7% at 6 hours and 18.8% at 8 hours. TA showed significant increases in cell viability when compared to NS-398 for all time points. These results are summarized in Figure 4.5.

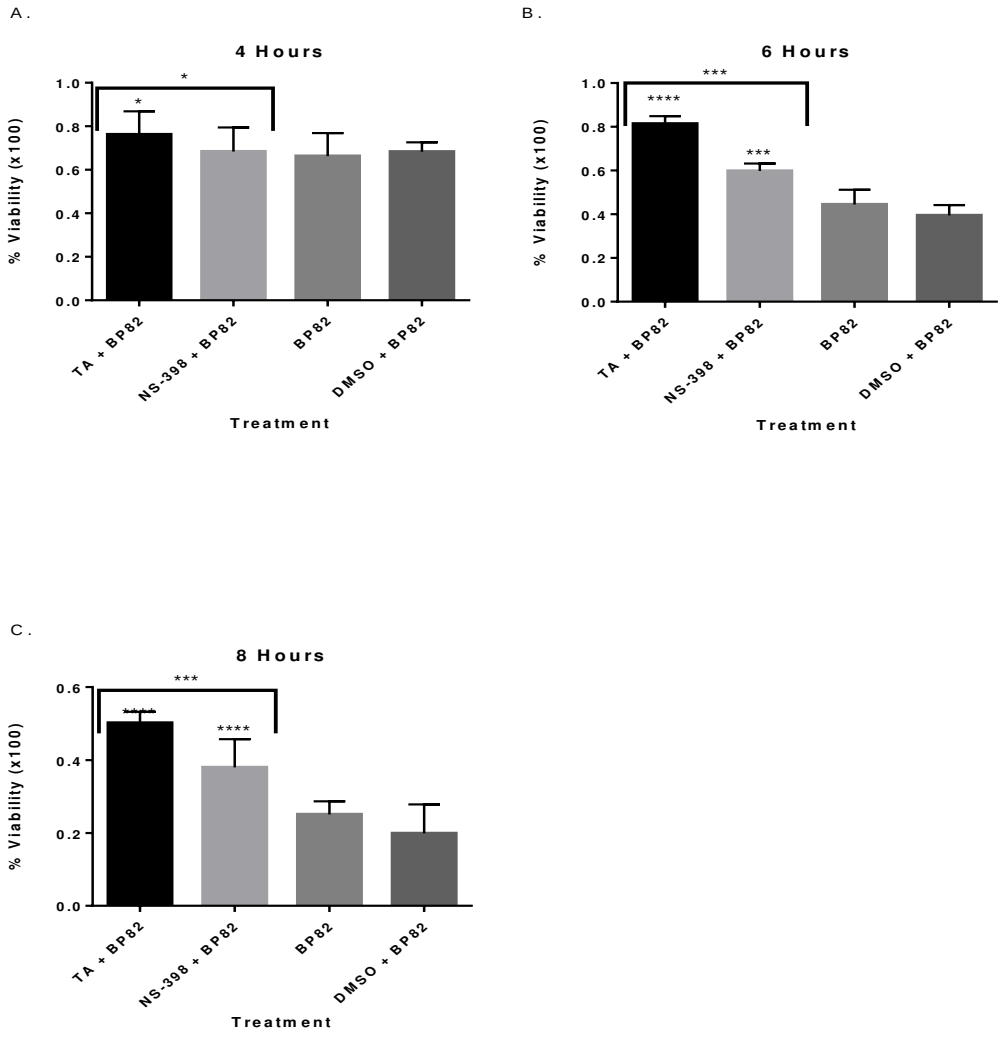

Figure 4.5. Effect of immune modulation on RAW 264.7 cell viability when infected with Bp82. For each time point, cells were pretreated for 30 minutes with 100µM TA, 100µM NS-398, 0.01% DMSO or were untreated and infected with a Bp82 MOI of 5. Cell viability was determined via optical absorbance at 570 utilizing the crystal violet method. Each treatment was normalized to uninfected/untreated control for each time point. The experiment was conducted in biological triplicate with ten technical replicates. Biological replicates were compared to the vehicle control via 2-way ANOVA with Bonferroni's post-hoc test for significance. A small significance was observed at 4 hours with TA treatment (A) where both 6 hours (B) and 8 hours (C) revealed a dramatic increase in cell viability with TA and NS-398 treatment. For all time points, TA treatment revealed a significant increase in cell viability when compared to NS-398. *$p<0.05$, ***$p<0.001$, ****$p<0.0001$

4.13 Discussion: Comparing NSAIDS

The results clearly show that both NS-398 and TA are effective at prolonging cell viability at four, six and eight hours post infection. More striking is that TA was significantly more effective at preventing cell death than NS-398 at all time points. It is difficult to compare these drugs directly as they are different classes of NSAIDS. While both have shown to inhibit COX-2, NS-398 is strictly known for its competitive inhibition of COX-2, where TA has a vast number of reported mechanisms for its effects on COX-2, prostaglandin production and other pathways that may be potentially of therapeutic value [26] [27]. These findings hint that there may be more to increasing cell viability than just lowering the production of PGE2 through COX-2 inhibition as reported in [2]. The next step was to determine if TA and NS-398 exhibit any inherent antibacterial properties by determining the minimum inhibitory concentration (MIC) of each of these inflammatory drugs on Bp82. This will help determine if the increase in cell viability seen is due to the drugs lowering the bacterial load through antibacterial properties or if other mechanisms are occurring.

4.14 Material and Methods: Minimum Inhibitory Concentration of NSAIDs on Bp82

In order to determine if the NSAIDs maintain any natural antibiotic properties within the dosing rage used in section 4.11, a MIC had to be established for each drug. As well as confirming the MIC for Ceftazidime, a known effective antibiotic against *B. pseudomallei*. To conduct this experiment, the MIC determination procedures outlined by Cummings *et al* (2013) [43] were used.

Bp82 stock was incubated in LB broth for 24 hours at 37°C and passed at a 1:100 dilution and incubated for an additional 6 hours. This stock was then diluted to reach an optical density at 600nm of 0.1 in caMHB. In 50µl of caMHB, 1:2 serial dilutions of NSAIDs and Ceftazidime were prepared in a 96-well plates with the highest concentration being 128µg/ml to the lowest concentration of 0.0625µg/ml, resulting in 12 dilutions. DSMO was also plated in 1:2 serial dilutions with 10% DMSO being the highest concentration down to 0.005%. 50µl of Bp82 sample was added to each well of the test plates. Additionally, 12 technical replicates of a positive control with only caMHB broth and Bp82 and a negative control with only caMHB broth were plated. MIC plates were incubated at 37°C with 5% CO2 for 18 hours at which point the plates were inspected visually for growth, using the positive and negative controls and indicators. Each treatment was run in triplicate and inspected by three different personnel for verification. The MIC concentration was determined as the lowest concentration of treatment that resulted in no bacterial growth.

4.15 Results: Minimum Inhibitory Concentration of NSAIDs on Bp82

The results in this experiment were incredibly consistent with little variation (see Table 1). Both TA and NS-398 did not exhibit complete inhibitory effects on Bp82 at any concentration tested. There was a noticeably smaller amount of Bp82 growth at 128 µg/ml of TA as compared to the positive controls although it was not enough to completely inhibit Bp82 growth. Ceftazidime exhibited a MIC at 4µg/ml.

TABLE 1. MIC of NSAID's and Antibiotics

Drug	Bp 82 MIC
TA	>489 µM [a]
NS-398	>407 µM [a]
Ceftazidime	7.31 µM [a]
DMSO	> 10%

[a] Concentrations converted to µM from µg/ml to maintain consistency with prior sections.

4.16 Discussion: Minimum Inhibitory Concentration of NSAIDs on Bp82

These data suggest that both TA and NS-398 do not possess any inherent antibacterial properties as the MIC are orders of magnitude greater than 100µM. This is important as it suggests the increase in cell viability seen in section 4.12 is not a result of the drugs causing cytotoxicity to Bp82 but is a result of some form of modulation of the RAW264.7 cells themselves. While this could be a result of immune modulation, as postulated in [2], the data is not sufficient to make that conclusion. In [2], MIC determination as not conducted; therefore, until now there was not sufficient evidence that therapeutic doses of NS-398 exerted an effect outside of COX-2 inhibition. Additionally, our experiment also revealed that the MIC of Ceftazidime is within the rage of previously reported values [43]. Finally, as for both NS-398 and TA the drug delivery vehicle was 0.01% DMSO. These results indicate that positive effects of both NS-398 and TA are not a result of DMSO. The next step is to determine why TA is so effective at improving cell viability after infection with Bp82 by investigating the effects on COX-2, NF-κB regulation and prostaglandin production

4.17 Materials and Methods: Effect of TA on COX-2 and NF-κB

For both flow cytometry and western blotting, two million RAW 264.7 cells were plated in three six-well plates for 24 hours. Cells were then washed two times with PBS (pH 7.4) pre-treated with 100µM TA or 0.01% DMSO for 30 minutes in complete DMEM. The untreated and uninfected control were pretreated with fresh media. After pre-treatment, cells were infected at an MOI of 5, and centrifuged for 5 minutes at 500 rpm to allow the bacteria to reach the monolayer. For NF-κB, cells were infected for 90 minutes where COX-2 samples were infected for 6 hours, the difference in time chosen was in order to maximize yields of these short lived inflammatory markers.

Preparation for flow cytometry analysis involved washing the cells two times with PBS (pH 7.4), removing them from the plate via trypsin and transferring them to a 15 mL conocal tube. Cells there then spun-down at 500 rpm for 5 minutes, the supernatant was removed, and the samples were fixed using a 3.7% formaldehyde solution in PBS for 20 minutes. The samples were then centrifuged at 500 rpm for 5 minutes. Samples were washed in PBS, isolated and re-suspended in 100 µL 0.1% triton 100-X in PBS solution for 10 minutes. 4 µL of either the COX-2 or NF-κB primary antibody was added directly to the sample and allowed to incubate for 20 minutes at 42°C. Samples were washed in PBS, spun down at 500 rpm for 5 minutes, re-suspended in 100 µL 0.1% triton 100-X in PBS. 2 µL of the secondary antibody conjugated to a fluora fuor was added to each sample and samples were allowed to stain for 20 minutes at 42°C. Samples were then washed in PBS, spun down at 500 rpm for 5 minutes and re-suspended in PBS in preparation for analysis on the flow cytometer. 5,000 events were collected per sample in duplicate across three biological replicates for statistical significance.

To prepare for western blotting, samples were washed two times with PBS (pH 7.4) and lysed using RIPA buffer with 0.1% protease inhibitor and lysed from the plate via scraping. Samples were sonicated and spun at 14,000*g* for 5 minutes. All samples were analyzed immediately or stored at -20°C. For protein quantification, the BCA assay was utilized (Thermo Scientific). Samples were run at 200 volts and blotted for 1 hour and 100 volts. Membranes were blocked in 5% milk in TBS for 30 minutes and the primary antibody was added in a 1:500 dilution and allowed to bind overnight. Membranes were washed three times in TBS-T blocked for 30 minutes in 5% milk in TBS and the secondary HRP antibody was added in a 1:1000 dilution for 1 hour. Samples were washed three times in TBS-T and WesternBright™ was added for detection on the Chemi-doc camera. Experiments were done in duplicate for statistical significance.

Immunofluorescence was prepared by plating 100,000 RAW 254.7 cells on a 12mm poly-L-lysin coated coverslip in a 24 well plate and cells were allowed 24 hours to adhere to the slide. Samples were pre-treated with 100µM TA or 0.01% DMSO for 30 minutes and infected at an MOI of 5 and previously described. For fixation and staining the protocol outlined in Miranda *et al* (2015) [44] was utilized. Briefly, cells were fixed in 2% paraformaldehyde for 15 minutes and blocked with BSA for 1 hour. Cells with primary antibodies were left overnight at 4°C and cells exposed to secondary fluora four antibodies incubated for 1 hour. DAPI was utilized for nuclear counter staining and slides were coverslipped for viewing.

4.18. Results: Effect of Tolfenamic Acid on COX-2 and NF-κB

Infection with Bp82 resulted in a 2-fold increase in COX-2 MFI from uninfected groups as presented in Figure 4.6. We also determined that pretreatment of RAW 264.7 cells infected with Bp82 with 100μm TA resulted in a ~30% reduction in COX-2 MFI versus the vehicle control group. Figure 4.7 offers a visual representation via immunofluorescence.

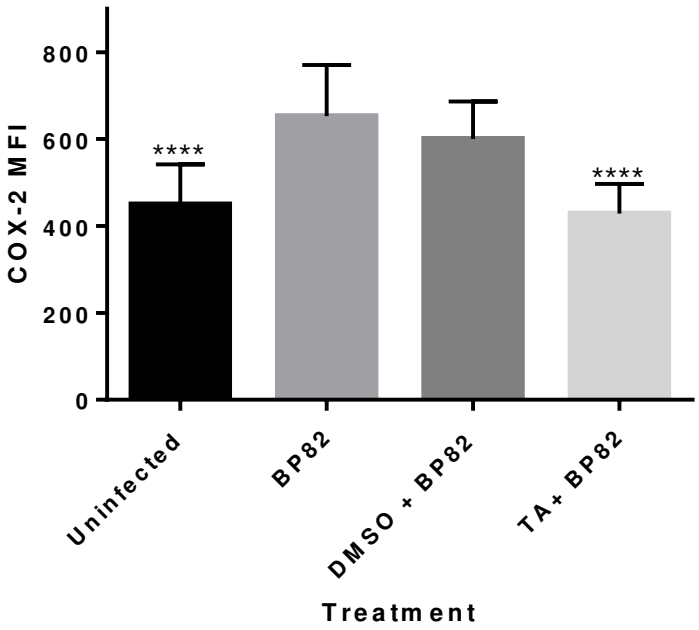

Figure 4.6. The effect of TA treatment on RAW 264.7 COX-2 expression when infected with Bp82 at 6 hours of infection. Cells were pretreated with 100 µM TA or 0.01% DMSO for 30 minutes along with an uninfected and untreated control. COX-2 levels were determined flow cytometry using the Mean Florescence Intensity (MFI) over 5,000 events. Significance was determined by comparing to the vehicle control, where TA treatment was able to suppress COX-2 expression significantly. Data is representative of three biological replicates run in duplicate. Significance was determined via 2-way ANOVA with Bonferroni's post-hoc test for significance. Error indicates SEM. ****$p<0.0001$.

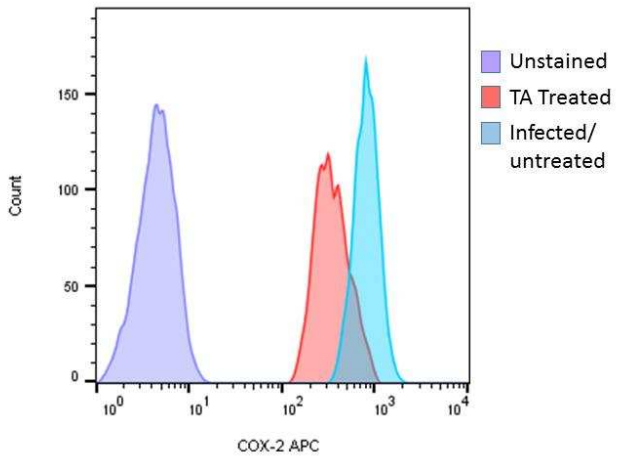

Figure 4.7. Visualization of MFI shift. Here, the unstained population falls within the first decade, where the infected and uninfected populations do not, indicating effective staining. The shift on the x-axis between the TA treated ground and the infected group indicate a decrease in MFI for TA treatment verse the infected group, revealing a decrease in COX-2 enzyme.

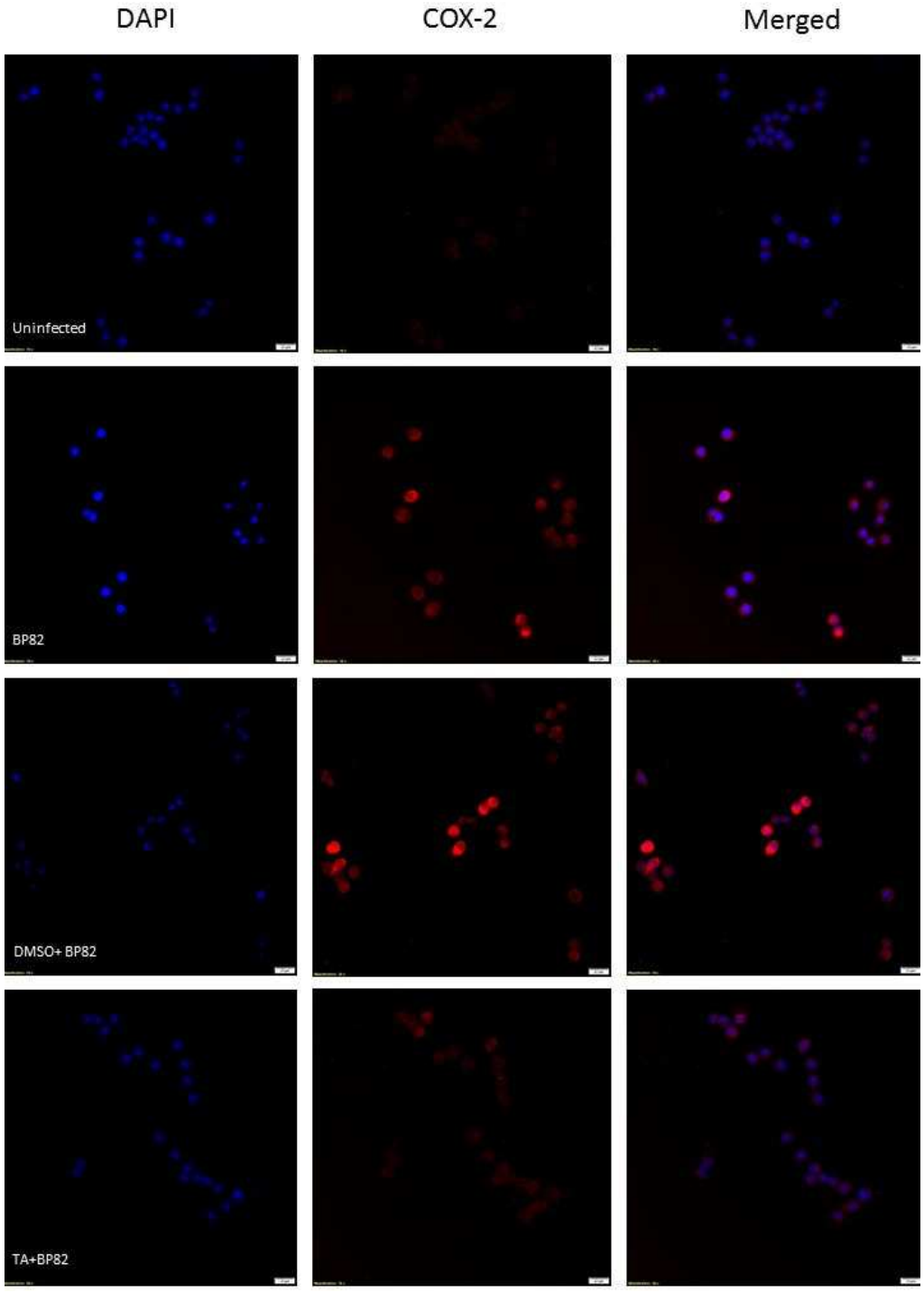

Figure 4.8. Effect of TA on COX-2 expression when infected with BP82 after 6 hours of infection. Cells were pretreated with 100 µM TA or 0.01% DMSO for 30 minutes along with an uninfected and untreated control. COX-2 levels were determined. Images are a visual representation.

Infection of RAW 264.7 cells with BP82 results in upregulation of NF-κB p65 indicating the activation of the NF-κB pathway. Infection resulted in a 2.5 fold increase in p65 MFI where pretreatment with TA resulted in a significant reduction of 20% MFI in p65. Unlike the COX-2, the vehicle control had no effect on p65 protein expression. These data are represented in Figure 4.9.

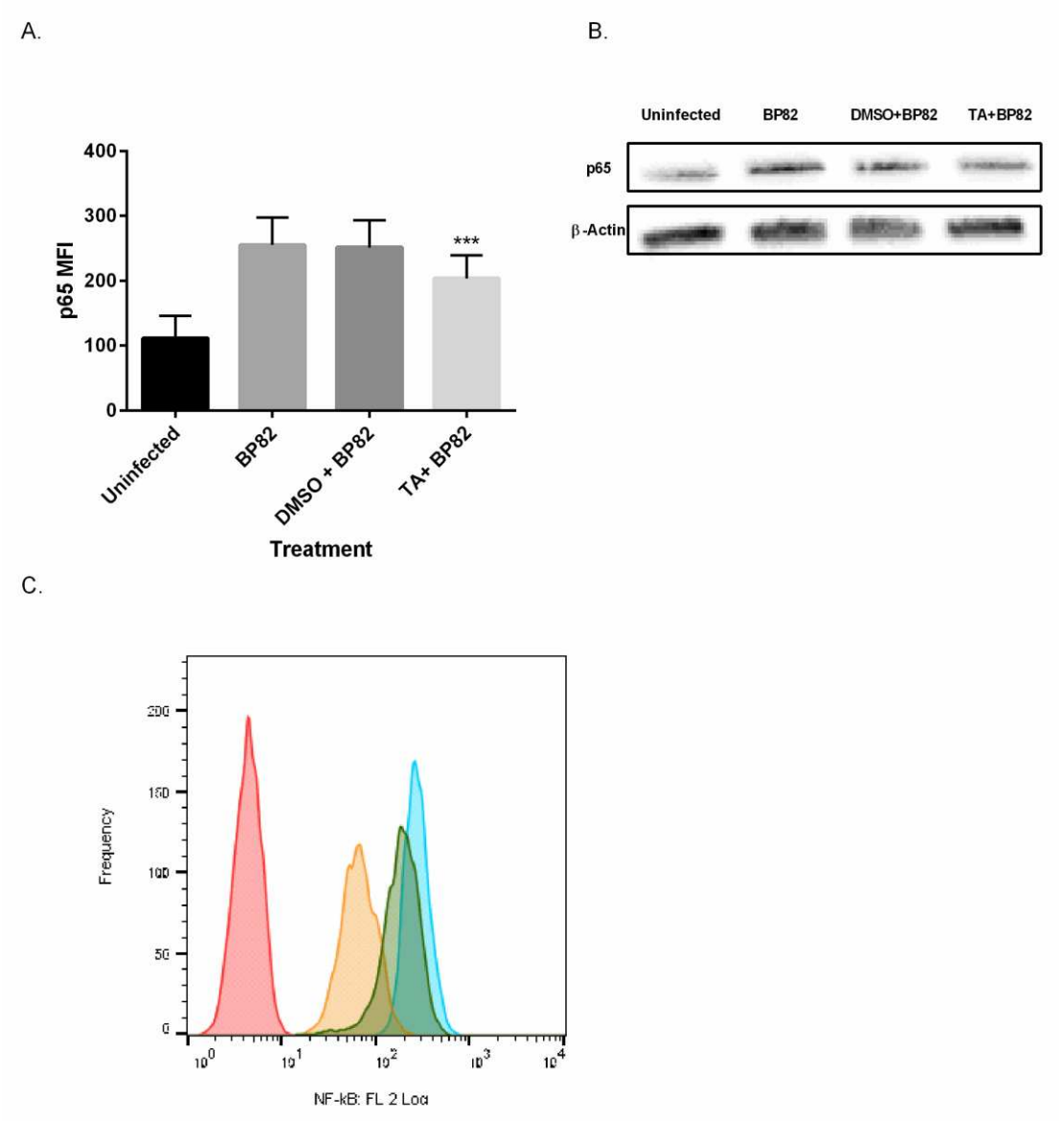

Figure 4.9. The effect of TA treatment on RAW 264.7 NF-κB p65 expression when infected with Bp82 after 90 minutes of infection. Cells were pretreated with 100 µM TA or 0.01% DMSO for 30 minutes along with an uninfected and untreated control. NF-κB p65 levels were determined flow cytometry using the Mean Florescence Intensity (MFI) over 5,000 events (A) with confirmation using western blotting (B). Significance was determined in (A) by comparing to the vehicle control, where TA treatment was able to suppress p65 expression significantly. (C) represents the data on a histogram. Data is representative of three biological replicates run in duplicate. Significance was determined via 2-way ANOVA with Bonferroni's post-hoc test for significance. Error indicates SEM. ***p<0.001, ****p<0.0001.

4.19. Discussion: Effect of TA on COX-2 and NF-κB

As TA is marketed as a COX-2 inhibitor, it is not surprising that it is able to significantly reduce COX-2 expression when infected with Bp82. What is unique to this study is that pretreatment with 0.01% DMSO had a significant reduction in COX-2 expression. While TA is a known anti-inflammatory agent that is known the reduce COX-2 expression [45], this was not used as a comparison in previous research utilizing NS-398 as the experimental NSAID [2]. TA revealed a significant reduction in COX-2 expression when compared to the vehicle control (DMSO). Additionally, the potency of TA as a COX-2 inhibitor can be seen when comparing levels to that of uninfected cells: samples treated with TA had a lower COX-2 expression than uninfected cells. This overall effect of TA on COX-2 indicates that TA would likely ffect PGE2 levels in a similar fashion.

As discussed in 2.4, TA has extreme variances in its effect on the NF-κB pathway depending on cell type and the source inflammation. Here, Bp82 infection significantly increased the expression of p65 and TA was able to significantly reduce that expression caused during infection. This is similar to the results in [20] where TA was able to reduce p65 activation during LPS stimulation in RAW 264.7 cells. Due to this reduction, treatment with TA could have profound impact on cytokine regulation and the overall magnitude of the inflammatory response during infection with Bp82. More research in needed in order to confirm this hypothesis.

4.20 Materials and Methods: Effect of TA on PGE2 Production

Two million RAW 264.7 cells were plated in a three six-well plates for 24 hours. Cells were then then washed two times with PBS (pH 7.4) pre-treated with 100µM TA or 0.01%

DMSO for 30 minutes in complete media. The untreated and uninfected control were pretreated with fresh media. After pre-treatment, cells were infected at an MOI of 5, and centrifuged for 5 minutes at 500 rpm to allow the infectious agent to reach the cell monolayer. At each time point after infection, the supernatant was removed and 1% BHT solution was added to avoid the free-radical peroxidation [42]. Samples were then analyzed immediately or stored at -20°C for later analysis. PGE2 analysis and quantification was conducted via ELISA using a PGE2 analysis kit (R&D Systems) in accordance with the manufactures instructions, except samples were not diluted as indicated. This experiment was conducted in three independent trials, each run in duplicate. Analysis of samples was conducted via 1 and 2 way ANOVA with Bonferroni's post-hoc test for significance.

4.21 Results: Effect of TA on PGE2 Production

Treatment of infected RAW 264.7 cells with TA significantly reduced the production of PGE2 *in-vitro*. After 4 hours, PGE2 levels were 4.4 times higher in the vehicle control group than in the group treated with TA. This was similar at other time points as TA was able to reduce PGE2 expression by five and six times after 6 and 8 hours, respectively. Also of interest, TA was able to lower PGE2 levels in infected media lower than that of uninfected media. The time course indicates an increase of PGE2 over time. For the infected control the PGE2 levels at 4 hours were 858 pg/ml where at 6 and 8 hours the level increased to 1162 pg/ml and 1708pg/ml, respectively. These results are summarized in Figure 4.10.

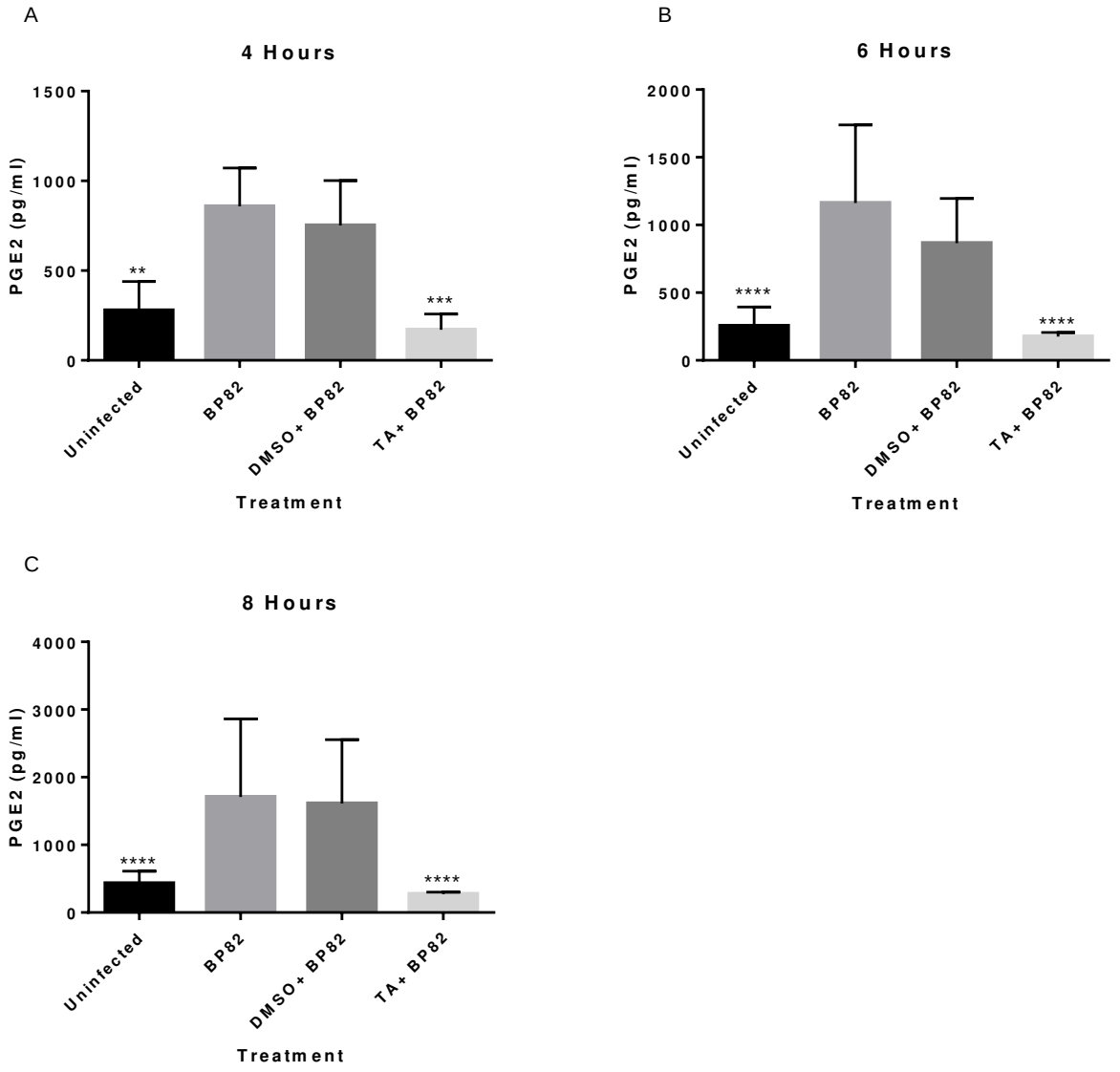

Figure 4.10. The effect of immune modulation on RAW 264.7 PGE2 production when infected with Bp82. For each time point, cells were pretreated with 100 µM TA or 0.01% DMSO for 30 minutes along with an uninfected and untreated control. PGE2 levels were determined via ELISA. Significance was determined by comparing to the vehicle control at all time points, where TA treatment was able to suppress PGE2 levels to below that of the uninfected control in all cases. Significance was determined via 2-way ANOVA with Bonferroni's post-hoc test for significance. Error indicates SEM. **p<0.01, ****p<0.0001.

4.22 Discussion: Effect of TA on PGE2 Production

The data presented above demonstrate the ability of TA to reduce the production of PGE2 during an infection with Bp82. The results are similar to those previously reported with NS-398 [2]; however, the two NSAIDS cannot be directly compared due to differences in experimental design. What is more interesting is that TA was able to reduce the PGE2 expression to level lower than baseline. It could be argued that this reduction could be due to cell death caused by treatment, however, data in section 4.12 clearly show that cell viability is actually increased at these time points with the same MOI. Additionally, the same result was observed in COX-2 expression in section 4.18. From this data, two very important conclusions can be drawn. First, BP82 infection increases the concentration of PGE2, suggesting the COX-2 pathway is involved in the response to infection. Second, TA is able to reduce PGE2 expression, most likely by inhibiting COX upstream during this infection.

Although the results were not significant when analyzed, there is a clear trend that DMSO at 0.01% concentration also reduces the level of PGE2 expression. When applied to the inflammatory process, this could be due to two main reasons. First, DMSO is a known anti-oxidant [46] [45] and may reduce oxidative damage generated in the inflammatory response. This effect was seen on the reduction COX-2 expression in section 4.18. Second, and of critical importance to the main hypothesis, DMSO has been shown to significantly reduce the activation of NF-κB P65 [22]. This reduction in activation could result in less transcription of inflammatory mediators that play a role in COX-2 expression.

4.23 Chapter Summary

In this chapter, a method to analyze cell viability utilizing CV for RAW 264.7 cells was optimized. This allowed for the identification of the optimal MOI of Bp82 to use for experiments throughout AIM 1. It was determined that pretreatment with TA is effective at prolonging increasing infected cell viability and the optimal dose of 100µM was identified. This optimal TA dose was then compared to the optimal dose of NS-398 identified in other literature where it was shown that TA is more effective at increasing cell viability than NS-398. The effects of TA on the inflammatory response of RAW 264.7 was shown to significantly reduce both COX-2 and p65 expression as well as reduce the production of PGE2. This data helped design and optimize the *in-vivo* experiments in Chapter 5.

CHAPTER 5: AIM 2

5.1 Chapter Introduction

The goal of this chapter is to extend the work obtained from the previous chapter into a live animal model using a lethal strain of *B. pseudomallei*; 1026B. To accomplish this, two animal studies were conducted. First was a control study, where animals were subjected to only drug treatments with no infection in order to achieve baseline values for experimental procedures. The second study used the same or similar treatments as the control study, but were infected with 1026B. The post-hoc studies included the NF-κB and COX-2 inflammatory markers of each animal in their peripheral blood mononuclear cells (PBMC's) using flow cytometry and colony forming units (CFU) counts in the lung, liver and spleen of infected animals.

5.2 Materials and Methods: Control Treatment Groups

For the treatment control studies, which did not include infection, the mice were divided into five different groups with five mice in each group. Group one was treated with 50 mg/kg of TA dissolved in 50µL of 100% DMSO given intraperitoneal (i.p). The side of the abdomen that received the dose altered with each treatment. It is important to note that 100% DMSO is not typically used as a vehicle as it has a tendency to be lethal to mammalian cells, however, this vehicle was used in previous experiments [2], and therefore, we replicated the process. Additionally, TA and NS-398 are only soluble in highly organic solvents, therefore, finding an alternative vehicle proved difficult. Group two was treated with 200 mg/kg ceftazidime

solubilized in PBS at pH 7.4. This was administered subcutaneously (s.c) in approximately 200µL (volume changed based on weight). Group 3 received 15 mg/kg NS-398 solubilized in 50µL of 100% DMSO i.p, similar to TA. Group 4 were treated with a combination of TA at 50 mg/kg i.p in 100% DMSO and 25 mg/kg ceftazidime given s.c. Group five was a vehicle control of 50µL 100% DMSO given i.p.

Mice were weighed prior to each treatment in order to determine treatment volume. Treatments occurred once every 24 hours and after 57 hours mice were euthanized via standard CO2 protocol. After this, blood was removed via intra-cardiac draw for analysis and the lungs, liver, and spleen were removed and placed into 10% formalin for further analysis.

5.3 Results: Control Treatment Groups

Not all treatment groups survived their treatment. Treatment groups that utilized 100% DMSO as a vehicle experienced increased death rates within 57 hours, however, the animals did not lose at least 20% of their initial body weight. Even more surprising is that death didn't occur the group treated with NS-398 which did use DMSO as a vehicle control. This data is represented in Figure 5.1A and 5.1B. The survival curves were split into two figures for simplicity.

A.

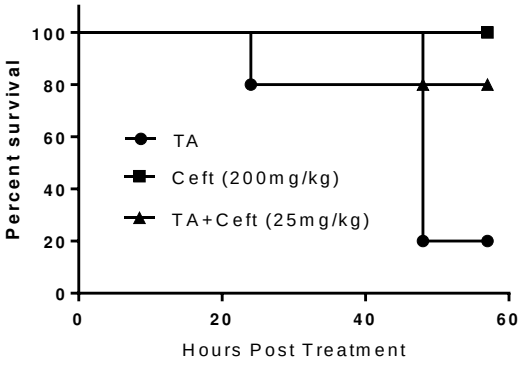

B.

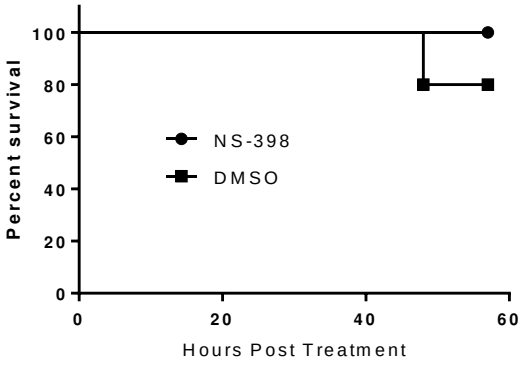

C.

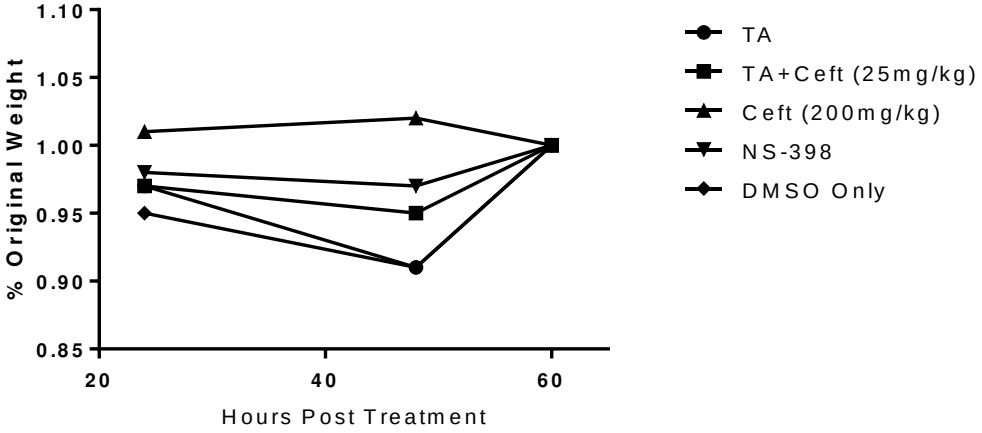

Figure 5.1. Survival curves for all treatment control groups separated into two survival curves (A and B) and the overall weight loss for the treatment control groups (C). Only groups that utilized DMSO as a vehicle for drug delivery, with the exception of NS-398, experienced death due to treatment alone. Additionally, all groups utilizing DMSO experienced some level of initial weight loss. This data confirms that DMSO is not an acceptable vehicle for TA treatments and another route should be utilized.

5.4 Discussion: Control Treatment Groups

The results above highlight the need for treatment control groups. If this experiment was done with infection initially, it would be unclear if the animals died due to the infection or the treatment. This highlights a potential error published by Asakrah *et al* (2013) [2], as uninfected vehicle control groups were never discussed. Therefore, it is unknown if the death seen during treatments was a result of the DMSO treatment or the infection. With the exception of the Ceftazidime treated group, all groups experienced initial weight loss with the DMSO control group loosing almost 10% in 48 hours. However, all groups returned to approximately their initial weight even though many of the animals died during treatment. Therefore, it is likely that those animals most effected by the treatment lost the majority of the weight while those unaffected maintained or even gained weight. Additionally, because less than 20% of the initial body weight was lost it is possible that the weight loss was due to the animal being under stress from treatment.

Our control study clearly showed the need for a different vehicle and route of treatment for TA as it cannot be administered by the same route as NS-398. What is also remarkable about these results is that while DMSO, TA and TA+ Ceftazidime group all experienced death due to the treatments, the NS-398 treatment group did not experience death or a significant weight loss. This indicates that NS-398 may effectively treat the damage caused by DMSO for at least a short period of time. The mechanism by which this occurs is unclear since both TA and NS-398 are both strong COX-2 inhibitors [34] [33]. More studies would need to be conducted in order to determine how NS-398 elicits its protective effects against DMSO.

5.5 Materials and Methods: Isolation and Analysis of PBMC's

In order to isolate the PBMC's from the whole blood, after blood was drawn, it was immediately placed into 10mL of a red cell lysis buffer at room temperature. The buffer was comprised of 8,209 mg/L Ammonium Chloride (Mallinckrodt Chemical Works), 1000 mg/L Potassium Bicarbonate (Fisher) and 37 mg/L of EDTA (Sigma). After 10 minutes the PBMC's were isolated via centrifugation at 500 rpm for 10 minutes. The supernatant containing the lysed red blood cells was removed and the PBMC pellet was re-suspended and washed in 1ml of sterile PBS. The sample was centrifuged again at 500 rpm for 5 minutes, after which, the PBMC's were re-suspended and fixed in 4% paraformaldehyde for 20 minutes. After fixation, the samples were centrifuged at 500 rpm for 5 minutes, the supernatant was removed, and the pellet was re-suspended in incubation buffer comprised of 0.1% bovine serum albumin (BSA) in PBS. One sample from each group was then processed for immunostaining immediately and all other samples were frozen at -80°C in accordance with Otto *et al* (2015) [48] until processing.

In order to perform the flow cytometric stain for the target proteins, each sample PBMC was divided evenly into three separate 15ml conical vials: one each for unstained control, NF-κB and COX-2. To stain for NF-κB and COX-2, each sample was spun at 500 rpm for five minutes, supernatant removed, and suspended in incubation buffer with the corresponding primary antibody at a 1:2000 dilution and allowed to sit at room temperature for one hour. The unstained sample was re-suspended in PBS and placed in 4°C refrigeration. After the primary antibody incubation, the sample was spun at 500 rpm for five minutes and washed with 2mL of incubation buffer, spun at 500 rpm for five minutes again, and re-suspended in a 1:2000 dilution of the secondary alexa fluor antibody in incubation buffer. This was allowed to stand at room

temperature for one hour in the dark. Cells were spun at 500 rpm for five minutes and washed with incubation buffer and then spun and re-suspended in PBS for analysis.

5.6 Materials and Methods: Flow Cytometry Settings and Gating

Previous research using similar methods has shown that the isolation of PBMC's using red blood cells lysis will result in three very distinct cell populations corresponding to the leukocytes, monocytes and granulocytes [49]. Any further identification within each population must be done by tagging the target cells within the population. For our purposes, further identification was not needed. Therefore, each population was identified using forward scatter versus side scatter plot and analyzed together and individually. The samples were then analyzed for their percentage of the cell population expressing the proteins of interest as well as the mean florescence intensity (MFI) to represent the level of expression.

5.7 Results: Control Group PBMC's Flow Cytometry Analysis

As the number of animals for this study were limited, any issues with the protocol would not be apparent until the final analysis. Initially, the flow analysis of the PBMC's were extremely promising as shown in Figure 5.2A. This is just one the five initial samples that showed extreme promise as the PBMC isolation procedure was confirmed to be effective. However, those samples that were cryopreserved in accordance with the procedures described previously [48], did not have the same result, as shown in Figure 5.2B. While Figure 5.2B does clearly reveal different cellular populations, the results from those samples that were frozen and those

processed immediately cannot be compared or utilized. Therefore, the baseline NF-κB and COX-2 percentage expression and MFI for all treatment groups only had one replicate, which is not statically significant. While this data cannot be used for definitive analysis, it still provides insight into the protein expression in these samples and serves as a good pilot study.

A B.

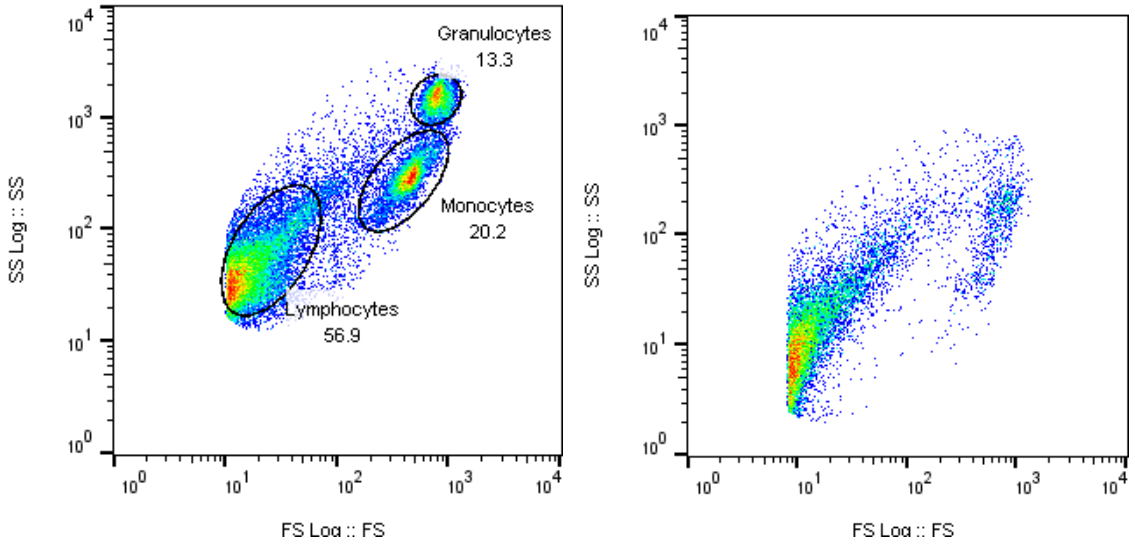

Figure 5.2. Results of flow analysis of PBMC in uninfected treatment control mice. The proper separation of PBMC's into its subpopulations of Lymphocytes, Monocytes and Granulocytes can be seen in (A), where (B) represents that result of cryopreservation on the samples. Both of the above samples were taken from difference mice in the same DMSO treatment control group.

5.8 Discussion: Control Group PBMC's Flow Cytometry Analysis

Unfortunately, due to the lack of successful freeze-back of the majority of the PBMC samples, this was a failed effort to determine the effect of treatments on PBMC as well as a failure to establish a baseline control by which to compare infected mice sample. However, these results clearly indicate that the procedure is successful when executed without a freeze-back and can be

used to isolate the three main populations of PBMC's. This confirmation of experimental protocol can be very useful and powerful tool for experiments in the future.

5.9 Materials and Methods: *In-Vivo* Infection with *B. Pseudomallei*

Due to the results of the control treatment study, a new group of animals was added and the route of drug administration was altered due to the resulting deaths described in section 5.4. All groups had 5 mice (n-=5/group). First, mice were anesthetized with 88 mg/kg ketamine i.p. and infected with approximately 2,000 CFU *B. pseudomallei* in 20 µL sterile saline. This was done dropwise in alternating nostrils. Animals were allowed to regain full consciousness and mobility for three hours, and then treated in accordance to their respective group. The mice in each treatment group were to be euthanized when the untreated control group began to show the signs of mortality described in section 3.4, in order to compare bacterial burden in the lung liver and spleen of each treatment group. Mice were weighed and administered treatment in accordance with the average cage weight. Group one was treated with 50 mg/kg of TA dissolved in 200µL of corn oil given orally as this is an alternative route with proven effectiveness for other applications of TA [32]. Group two was treated with 200 mg/kg ceftazidime solubilized in PBS at pH 7.4. This was administered subcutaneously (s.c) in approximately 200µL of solution (volume changed based on weight). Group 3 was administered 15 mg/kg NS-398 solubilized in 50µL of 100% DMSO i.p as this treatment group experienced no mortality. Group four was administered a co-treatment of TA at 50 mg/kg orally in corn oil and 25 mg/kg ceftazidime given s.c. and group five was only given 25 mg/kg ceftazidime s.c. Group six was untreated and group 7 was a vehicle control of 200µL corn oil only.

After the first treatment, animals remained in standard conditions described in section 3.4, and were weighed and treated every 24 hours for two additional treatments, resulting in three total treatments in 51 hours. After which, animals were weighed every 12 hours and monitored for signs of mortality.

Once the untreated control group began to exhibit signs of mortality, all mice were anesthetized by administering 88mg/kg of ketamine i.p. Intra-cardiac blood draws were done as described in section 5.5. This draw prior to euthanasia provided a larger quantity of blood for the analysis of PBMC's as described in section 5.5. Mice were then euthanized via cervical dislocation and necropsied, removing the lung liver and spleen of each animal. Organs from three mice in each treatment group were homogenized in sterile saline and plated on LB agar in serial dilutions in duplicate, incubated at 37°C for 48 hours and counted for CFU's to determine bacterial burden. The organs from the remaining two mice in each treatment group were preserved in 10% formalin solution for later historic analysis.

5.10 Results: *In-Vivo* Infection with *B. Pseudomallei*

The infected control group exhibited signs of mortality at 60 hours post-infection, so, all mice in all groups were euthanized within 1 hour. Weight loss within this group reached 20% (Figure 5.3) as well as a hunched appearance, and almost complete lack of response to stimuli. This was mimicked by the corn oil treatment (vehicle control) group that was also infected. All other groups exhibited weight-loss, but still maintained a generally healthy appearance given their infection.

The PBMC analysis revealed no significance due to improper lysis of the red blood cells and/or preservation of the PBMC's. Unlike the control treatment group, none of the PBMC samples were cryopreserved, however, the resulting flow analysis for all samples showed results similar to that in Figure 5.2B. While extensive analysis was attempted on these results, no significant or reliable data was acquired.

1026b CFU counts revealed substantial variation between the treatment groups and organ CFU burden as shown in Figure 5.4. In the lung, only 200 mg/kg of Ceftazidime was able to substantially reduce bacterial burden. All groups except the 200 mg/kg Ceftazidime group revealed a lung burden that was orders of magnitude above the initial inoculation dose. The liver burden was substantially reduced in those groups treated with 200 mg/kg Ceftazidime and the co-treatment of TA and 25 mg/kg Ceftazidime. The spleen data was interesting in that all forms of treatment, with the exception of 25 mg/kg Ceftazidime, showed a reduction in CFU burden. However, this reduction was also visible in the corn oil (vehicle control) group, therefore, the only significant reduction in burden was found in 200 mg/kg Ceftazidime group since statistical analysis was conducted using the corn oil group as the comparative control. Note, that there is no liver data from the 25 mg/kg group as this experiment was done separately, under the same conditions, and the livers were not taken for CFU burden determination.

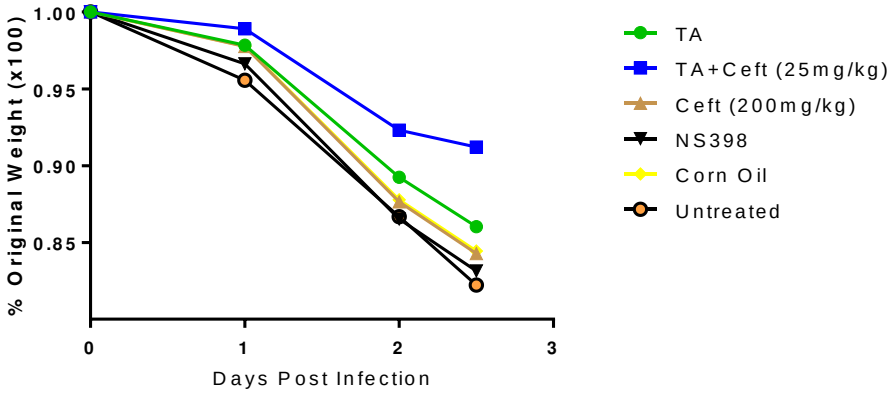

Figure 5.3. Weight loss exhibited by the treatment groups over the course of 2.5 days. BALB/c mice (n=5 per group) were infected with 2 X 10^3 CFU (~4 X LD50) of B. pseudomallei 1026b intranasally. Three hours post-infection treatments were administered, then again daily for two consecutive days totaling three treatments. Group 1 was administered 50mg/kg TA orally in corn oil, Group 2 was co-treated with 50mg/kg TA plus 25 mg/kg ceftazidime subcutaneously in PBS, Group 3 administered 25 mg/kg ceftazidime subcutaneously in PBS (data not shown), Group 4 was administered 200 mg/kg ceftazidime in PBS, Group 5 was administered corn oil as a vehicle control, and Group 6 was untreated.

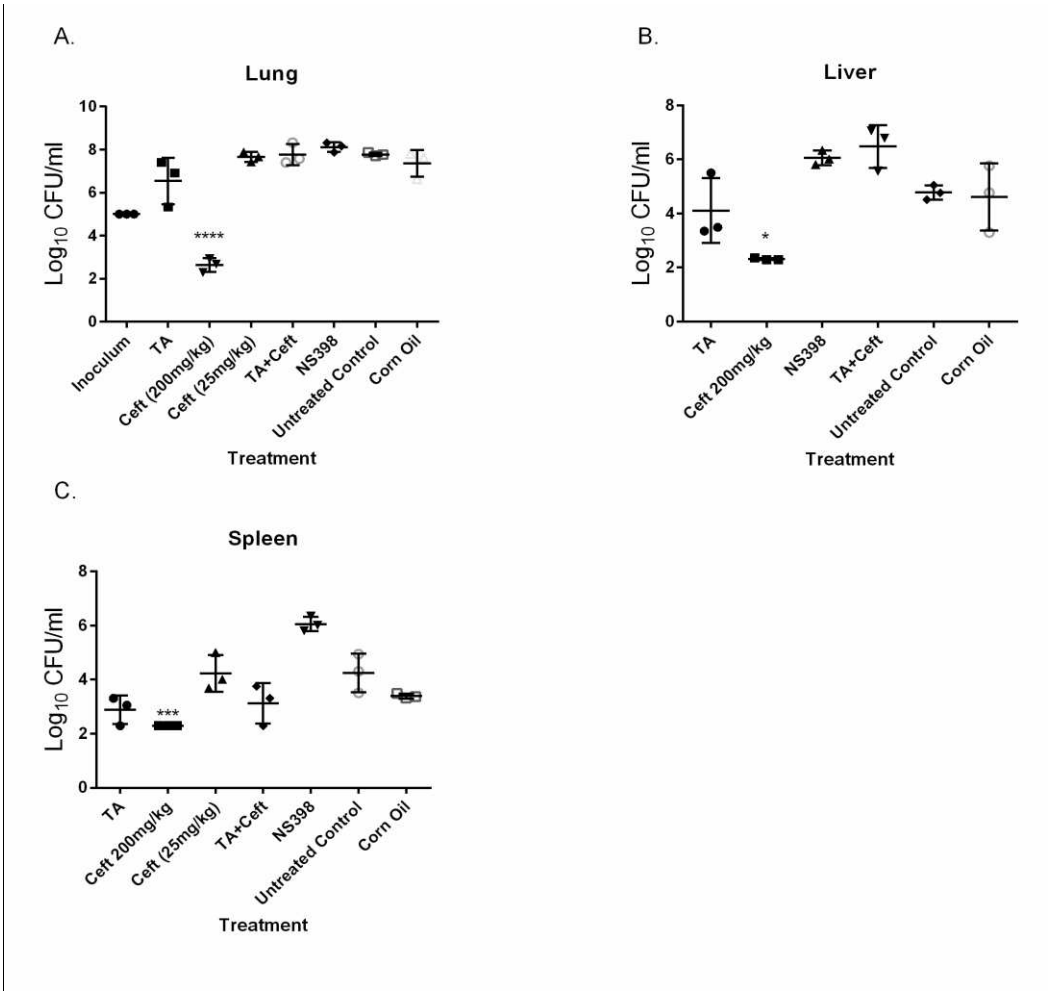

Figure 5.4. Comparison of the CFU burdens with various treatments in the lung, liver, and spleen after a lethal pulmonary infection of 1026b after 60 hours. BALB/c mice (n=5 per group) were infected with 2 X 10^3 CFU (~3 X LD50) of B. pseudomallei 1026b intranasally. Three hours post-infection treatments were administered, then again daily for two consecutive days. Treatments included: 50mg/kg TA orally in corn oil, a co-treatment of 50mg/kg TA and 25 mg/kg ceftazidime subcutaneously in PBS, 25 mg/kg ceftazidime subcutaneously in PBS, 200 mg/kg ceftazidime in PBS, corn oil as a vehicle control, and untreated. Organ homogenates were plated in serial dilution in duplicate and compared to Group 5 (vehicle control) for significance using a 1-Way ANOVA with Bonferroni's post-hoc test for significance. Only the 200mg/kg Ceftazidime treatment was able to significantly reduce CFU burden in the lung, liver and spleen (A-C),. The inoculum dose is included in the lung data (A) for comparison. Data is representative of 3 animals per group. LOD indicates the limit of detection using the logarithmic scale. Error indicates SD. Note, Group 3 does not have any liver data. *$p<0.05$, ***$p<0.001$, ****$p<0.0001$.

5.11 Discussion: *In-vivo* Infection with *B. Pseudomallei*

It is possible that the analysis of PBMC's failed due to a mistake in the experimental design. This was likely due to varying times the blood had to remain in lysis buffer. The high number of animals that had to be euthanized paired with limited resources and workspace within the BSL-3 resulted in the blood samples being in the lysis buffer for a period often exceeding ten minutes. This likely resulted in the lysis of the PBMC's along with the red blood cells leading to the poor result seen. The method of PBMC collection is still valid and the technique could still be used to provide a vast amount of knowledge regarding the response of PBMC's during melioidosis. This protocol should be optimized further and attempted again as it may yield useful knowledge for further treatment.

It is hard to make a clear determination about the efficacy of each treatment based on the bacterial burdens since the CFU counts did not show significant reductions with immune modulation. The only treatment that produced the expected results was the 200 mg/kg ceftazidime group as reduction in the lung and spleen to near the limit of detection is common [50]. However, when looking at the CFU burden in the spleen, there is a clear association between the treatment of TA (both groups) and reducing the spleen burden. While this is not significant when analyzed mathematically, this trend may be important. Although this data, by itself, is not entirely convincing of the efficacy of TA to fight *B. pseudomallei* infection, this data paired with the effect of TA on cell viability and the reduction of the immune response through COX-2 and NF-κB pathways shown in Chapter 4 do provide significant evidence for the effectiveness TA. Based on the CFU counts, the dissemination of *B. pseudomallei* appears to disseminated from the lungs, to the liver and finally to the spleen.

5.12 Materials and Methods: Survival Study for In-Vivo Infection with *B. Pseudomallei*

To reduce the number of animals used, this experiment was done in conjunction with the previous experiment outlined in section 5.9. BALB/c mice divided randomly into five groups (n=5/group) were anesthetized with 88mg/kg ketamine i.p. and infected with approximately 2,000 CFU *B. pseudomallei* in saline. This was done dropwise in alternating nostrils. Animals were allowed to regain full consciousness and mobility for three hours, and then treated in accordance to their respective group. Mice were weighed and administered treatment in accordance with the average cage weight. Group one was treated with 50 mg/kg of TA dissolved in 200µL of corn oil given orally. Group two was administered 15 mg/kg NS-398 solubilized in 50µL of 100% DMSO i.p. Group three was administered a co-treatment of TA at 50 mg/kg orally in corn oil and 25 mg/kg ceftazidime given s.c. and group four was only given 25 mg/kg ceftazidime s.c. In effort to reduce animal use, there was no 200 mg/kg Ceftazidime survival study as a significant amount of research indicates that this treatment is effective for at least 30 days post infection [43].

After the first treatment, animals remained in standard conditions described in section 3.4, and were weighed and treated every 24 hours for two additional treatments for a total of 3 treatments in 51 hours. Animals were then weighed every 12 hours and monitored for signs of mortality. Once the infected but untreated and vehicle control group were euthanized due to signs of mortality, the time of survival for the treatment groups began. While the 25 mg/kg treatment group data was gathered from a separate experiment, all the conditions were identical to this experiment. Due to the prolonged survival of one particular group, this group was allowed to continue to live for 37 days, until it was decided to humanely euthanize the group and determine the bacterial burden within the organs as described in section 5.9.

5.13 Results: Survival Study for *In-Vivo* Infection with *B. Pseudomallei*

All but two treatment groups experienced significant weight loss from their original weights in a manner that was consistent with the data presented in section 5.10. The TA treatment group did not experience significant weight-loss, nor did they exhibit the extreme signs and symptoms outlined in section 3.4. However, the animals were mistakenly euthanized. The co-treatment of TA and 25mg/kg of Ceftazidime also did not experience weight-loss greater than 20%. These results summarized in Figure 5.5.

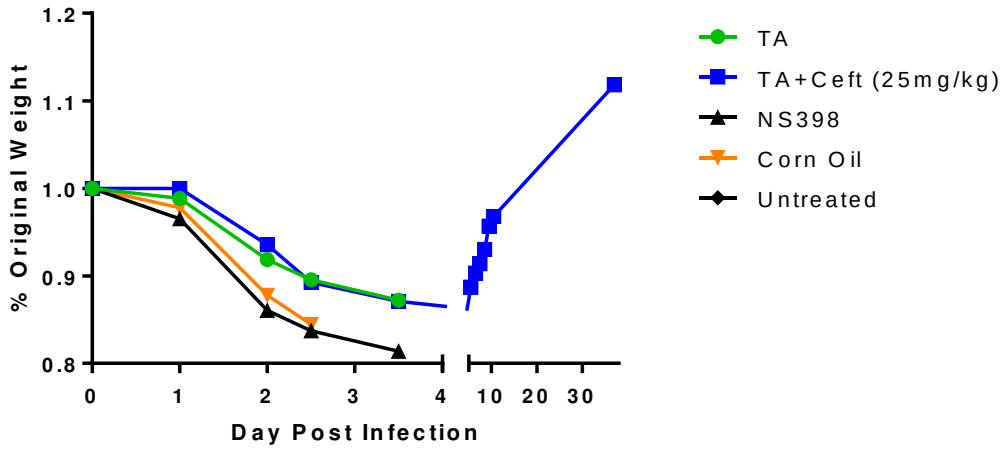

Figure 5.5. Weight loss exhibited by the survival treatment groups over the course of 2.5 days. BALB/c mice (n=5 per group) were infected with 2 X 10^3 CFU (~3 X LD50) of B. pseudomallei 1026b intranasally. Three hours post-infection treatments were administered, then again daily for two consecutive days totaling three treatments. Treatments included 50mg/kg TA orally in corn oil, co-treatment of 50mg/kg TA and 25 mg/kg ceftazidime subcutaneously in PBS, 25 mg/kg ceftazidime subcutaneously in PBS (data not shown), corn oil as a vehicle control, and untreated.

As indicated by the weight loss information above, some treatment groups survived longer than others. Of the survival groups, the groups infected but treated with corn oil, 25 mg/kg Ceftazidime, or the untreated control, all experienced mortality or showed signs of mortality outlined in section 3.4 after 2.5 days post infection. The group treated with NS-398 experienced a stepwise mortality, with one mouse experiencing mortality 2.5 days after infection, two more after three days post infection, one and 3.5 days post infection and the last mouse experiencing at 3.5 days post infection. The TA group also experienced stepwise mortality, but a slightly longer life expectancy: three mice died three days post infection with the remaining two mice being prematurely euthanized after 3.5 days post infection. The TA + Ceftazidime group experienced no mortality until they were euthanized after 37 days post infection to determine the organ bacterial burden. There were no signs of mortality at this point. It should be noted that one mouse in the TA + Ceftazidime group was cannibalized four days post infection, however, this death was not a result of melioidosis, so, the mouse was removed from the data. This data is summarized in Figure 5.6.

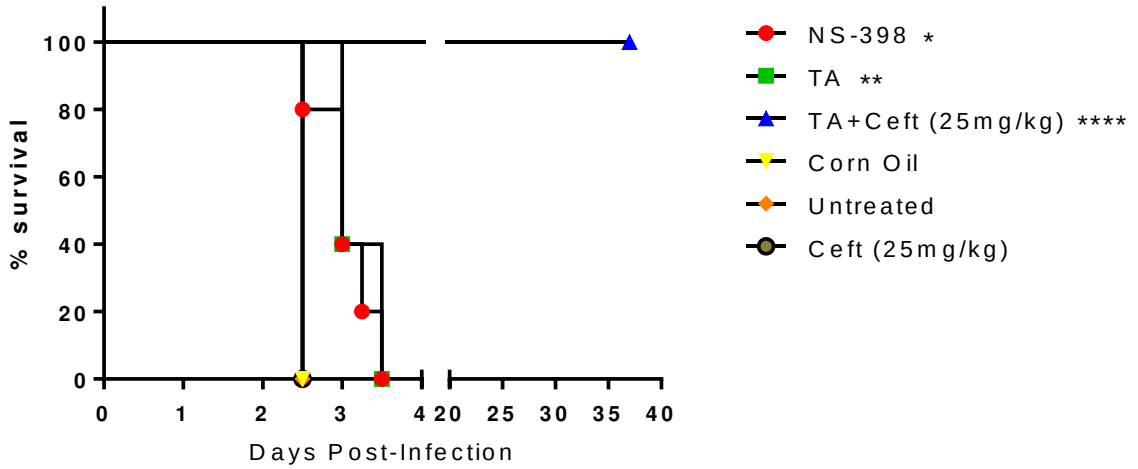

Figure 5.6. TA treatment and co-treatment of TA with a sub-therapeutic antibiotic treatment provides significant protection against lethal pulmonary Melioidosis. BALB/c mice (n=5 per group) were infected with 2 X 10^3 CFU (~3 X LD50) of *B. pseudomallei* 1026b intranasally. Three hours post-infection treatments were administered, then again daily for two consecutive days totaling three treatments. Group 1 was administered 15 mg/kg NS-398 s.c, group 2 was administered 50mg/kg TA orally in corn oil, Group 3 was administered 50mg/kg TA plus 25 mg/kg ceftazidime subcutaneously in PBS, Group 4 was administered 25 mg/kg ceftazidime subcutaneously in PBS, Group 5 was administered corn oil as a vehicle control, and Group 6 was untreated. Survival was monitored for 37 days. Statistical significance was determined via the Mantel-Cox test. *p<.05, **p<0.01, ****p<0.0001.

After 37 days post infection with 1026b, the bacterial burden was not completely eliminated from all the organ tissues in all mice that were treated with TA and a subtherapeutic dose of Ceftazidime. Each mouse had variability within each organ systems, with one mouse having complete clearance on *B. pseudomallei* in all organs analyzed, another mouse with detectable levels only in the spleen with clearance in the lungs and liver, and the last mouse with detectable CFU's in all organ tissue. The data represented in Figure 5.7 is the average throughout the population, but it is important to note the variability within the population as a whole.

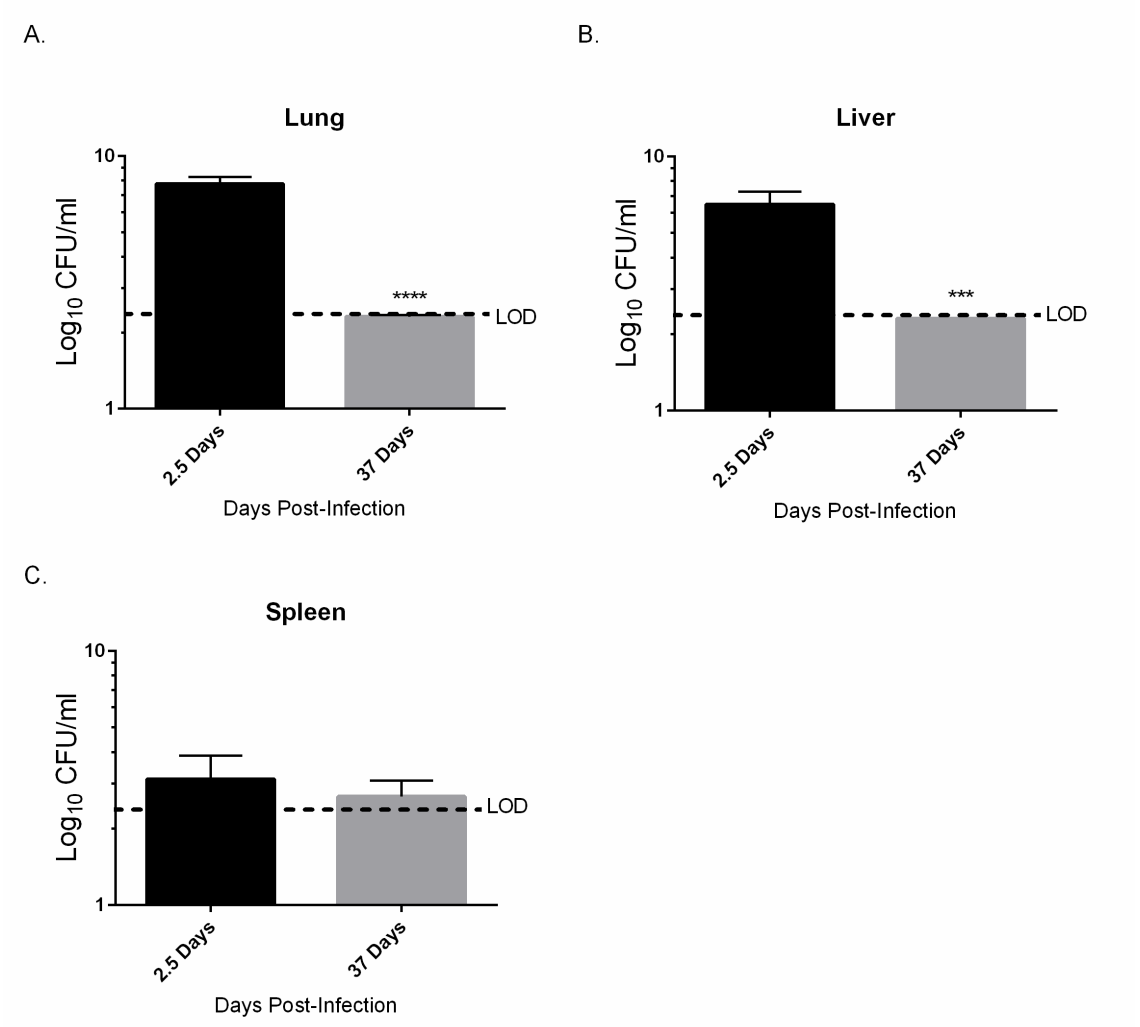

Figure 5.7. Co-treatment with TA sub-therapeutic Ceftazidime treatment may present a novel treatment for Melioidosis. After 37 days post-infection without indication of mortality from 4 X LD50 inoculation with *B. pseudomallei* 1026b with only three consecutive treatments in two days, the mice (n=3) were sacrificed to determine the bacterial burden in the lung, liver and spleen. These organs were removed, homogenized and plated in serial dilutions in duplicate. This data was then compared to the same treatment group at 2.5 days post-infection to determine if there was a significant reduction in bacterial burden over time. The lung (A) and the liver (B) both showed significant reduction in bacterial burden in the 35 days after treatment was terminated. The spleen (C) did experience a reduction in CFU burden, however, this was determined not to be significant. Samples were analyzed via two tailed t-test. Error indicates SD. ***$p<0.001$, ****<0.0001.

5.14 Discussion: Survival Study for *In-Vivo* Infection with *B. Pseudomallei*

The weight loss seen between the survival experiment and the bacterial burden experiments conducted in section 5.10 were consistent. This indicates the infection and the infectious dose was consistent between the two separate experiments and can be compared to each other for analysis.

While treatment with NS-398 did significantly prolong life when compared to the untreated group, this increased life expectancy was not as significant as seven days previously reported with the same treatment and treatment protocol by Asakrah *et al* (2013) [2]. This could be due to variations in the infectious dose as the dose used in this experiment was 2 X 10^3 CFU and the dose used in the previously reported experiment was 3 X 10^3 CFU. These doses represent approximately three and four times the LD50 for 1026b [2], respectively. Regardless of the rational for the lack of NS-398 result replication, we were able to show that treatment with TA alone was more effective at increasing life expectancy than NS-398. However, what is unclear is how significant this difference is. As mentioned in the previous section, the group treated with TA was euthanized prematurely due to a miscommunication between the Lab Animal Resources and the study personnel. After 3.5 days post infection, the remaining mice in this treatment group had only lost 10% of their initial body, which was consistent with the TA + Ceftazidime group. Although the TA treated mice did appear to be extensively sick as compared to the other remaining treatment group, they did not meet the criteria established to determine mortality. That is, these animals were still responsive to stimuli, did not have a hunched appearance, and had not lost 20% of their initial body weight. However, due to conflicting personalities and pressure from Lab Animal Resources, these animals were euthanized before the study design personnel could

respond to concerns. Therefore, while it is clear the TA is an effective treatment it is unclear how much more significant it is compared to treatment with NS-398.

The most significant results came from the group co-treated with TA and a sub-therapeutic Ceftazidime. In a separate study, we confirmed that treatment with 25mg/kg of Ceftazidime was not effective at preventing mortality in BALB/c mice with acute melioidosis. However, by modulation the immune response with TA, this treatment became successful. What is more astonishing is that the mice were able to survive 37 days with only 3 initial treatments. Additionally, the bacterial burden compared at 2.5 days post infection and 37 days post infection revealed that the host was almost able to clear the infection from its system, with one of the three mice analyzed being completely cleared of any bacterial burden. The success of this treatment leaves many questions to be answered. The fact that all other treatment groups experienced mortality between 2.5 and 3.5 days as well as the weight loss experienced by this treatment group reveal that the infection was successful. Is the slight bacterial burden remaining in the host all that is left of the infection? Or was the disease on the verge of relapse, which is common in Melioidosis, particularly when antibiotic treatment regimens are not completed [4]? TA has been shown to module the immune response through a variety of mechanisms, so, which mechanism is the most important? Previous reports indicate the reduction of PGE2 may play a critical role, however, if that were the sole case then the results between TA and NS-398 would be more similar in their effectiveness.

5.15 Chapter Summary

In this chapter, we revealed that there are several experimental errors in previously reported work, such as DMSO not being an effective vehicle for drug delivery when given i.p. as it can cause death within 48 hours. It was shown that treatment with TA and a co-treatment of TA and sub-therapeutic Ceftazidime results in a significant increase in survival outcome. Unlike previously reported work [2], we were unable to shownthat treatment with either TA or NS-398 did not significantly reduce the bacterial load in the lung, liver and spleen after 60 hours of infection. However, while co-treatment of TA and a sub-therapeutic dose of Ceftazidime did not significantly reduce the bacterial load in all organs after 60 hours of infection, it did allow for a substantial increase in survival which resulted in almost complete clearance of 1026b from the lung, liver and spleen after 37 days. Finally, while we were not able to obtain any significant information from PBMC analysis, we have shown that it is a valuable technique with extreme potential.

CHAPTER 6: FUTURE WORK

6.1 Chapter Introduction

As with most work on this nature, the results of this research have generated more questions than answers. The ways in which to approach the future work is almost limitless, so the most important focal points will be addressed.

6.2 Further Elucidating the Inflammatory Response

This study focused on COX-2 and NF-κB expression as well as PGE2 production. Both of the COX-2 and NF-κB pathways are very complex with multiple downstream products. In the appendix of this work, there are pilot studies which indicate TA may have a profound impact on cytokine production through the regulation of NF-κB. However, many other inflammatory pathways such as the c-Jun N-terminal kinases (JNK) pathway can also be investigated as to their response to *B. pseudomallei* infection and how treatment with TA affects this pathway.

6.3 Replication and Enhancement of the *in-vivo* Studies

While the impact of the *in-vivo* work is potentially substantial with the indication of a possible effective novel therapeutic strategy, replication of these results is needed to confirm the effectiveness of both TA and the co-treatment of TA and sub-therapeutic Ceftazidime. Additionally, the only effective post-mortem studies on the BALB/c mice was the bacterial load and dissemination with and without treatment. Additional studies, such as monitoring the level

peripheral cytokine levels, would help characterize the effects of treatments and why it has been so successful. Finally, while post-exposure treatment has proven effective, prophylactic treatment should also be investigated using TA, as this could prove to be using during a possible bio-terror threat.

6.4 Effectiveness of Treatment with Other Infectious Organisms

While *B. pseudomallei* has a significant global impact as well as potential as a bio-terror threat as indicated in section 2.1, there are other gram-negative organisms with a similar if not greater global burden. These include, but are not limited to, such organisms as *F. tularensis and M. tuberculosis* (although not strictly gram-negative). Effective treatment or enhancement of current treatments of these infectious diseases using TA could have a drastic impact on disease progression and the social-economic burden seen with infectious disease.

CHAPTER 7: CONCLUSION

Previous research concluded that inhibiting PGE2 production via COX-2 inhibition during *B. pseudomallei* infection was effective at increasing survival outcome in BALB/c mice. It was our hypothesis that altering the NF-κB pathway utilizing an NSAID that had a documented history of altering both the COX-2 and NF-κB pathway would prove an effective therapeutic for Melioidosis. Emphasizing that NF-κB expression was more important to increasing survival outcome. This research did not support my original hypothesis. While TA was shown to significantly decrease NF-κB expression during infection, it cannot be concluded that the NF-κB pathway was the most important. However, because the COX-2 and NF-κB pathways have known interaction during inflammationas outlined in section 2.3 it appears the NF-κB pathway does play an important role. While the main hypothesis was not well supported, through this research several significant discoveries manifested:

- TA was able to significantly increase cell viability *in-vitro* during infection with the *B. pseudomallei* surrogate Bp82
- Bp82 was shown to induce the COX-2 and NF-κB pathways in RAW 264.7 cells, validating its use as a BSL-2 surrogate to 1026b for monitoring the inflammatory response during infection.
- TA was shown to alter two inflammatory pathways by reducing NF-κB and COX-2 expression during infection with Bp82. The reduction in COX-2 resulted in a corresponding reduction of PGE2 production.

- We identified experimental errors in previously published work. These included the lack information on how DMSO altered the inflammatory response of COX-2 expression and PGE2 production, and how DMSO is lethal to BALB/c mice within 48 hours in the same experimental design. Additionally, we were not able to replicate the *in-vivo* results utilizing NS-398 in [2].
- Three consecutive treatments of TA treatment alone was able to significantly increase survival outcome in BALB/c mice, but it was not able to reduce spleen and liver bacterial burden after 60 hours.
- Three consecutive co-treatment of TA and sub-therapeutic Ceftazidime were also unable to consistently reduce organ bacterial burden after 60 hours post infection, however, this treatment was able to substantially increase survival outcome and almost completely clear the bacterial burden in the lung, liver and spleen after 37 days.

The results presented here prove useful supporting immune modulation using an oral dose of TA as a therapeutic to treat or enhance treatment of the acute, highly fatal disease Melioidosis. Continued research in immune modulation and the effectiveness of TA during Melioidosis are imperative to determining if this treatment can be effective in human cases of the disease.

CHAPTER 8: ORIGINAL CONTRIBUTION

8.1 Publications in Progress

One publication is likely to result from my graduate work. The results of this thesis as a whole will be submitted for peer review in April 2016.

REFERENCES

1. Select Agent and Toxins, Federal Register Part III, 42 CFR Part 73. (2015, September 10). Retrieved September 17, 2015.

2. Asakrah, S., Nieves, W., Mahdi, Z., Agard, M., Zea, A., Roy, C., & Morici, L. (2013). Post-Exposure Therapeutic Efficacy of COX-2 Inhibition against Burkholderia pseudomallei. *PLoS Negl Trop Dis PLoS Neglected Tropical Diseases, 7*(2), 2212-2212. doi:10.1371/journal.pntd.0002212.

3. Welkos, S., Klimko, C., Kern, S., Bearss, J., Bozue, J., Bernhards, R., Cote, C. (2015). Characterization of Burkholderia pseudomallei Strains Using a Murine Intraperitoneal Infection Model and In Vitro Macrophage Assays. *PLoS ONE PLOS ONE, 4*(10), 1-24. doi:10.1371/journal.pone.0124667.

4. Wiersinga, W., Poll, T., White, N., Day, N., & Peacock, S. (2006). Melioidosis: Insights into the pathogenicity of Burkholderia pseudomallei. *Nature Reviews Microbiology Nat Rev Micro, 4*, 272-282. doi:10.1038/nrmicro1385.

5. Currie, B., Ward, L., & Cheng, A. (2010). The Epidemiology and Clinical Spectrum of Melioidosis: 540 Cases from the 20 Year Darwin Prospective Study. *PLoS Negl Trop Dis PLoS Neglected Tropical Diseases, 4*(11). doi:10.1371/journal.pntd.0000900.

6. Limmathurotsakul, D., Golding, N., Dance, D. A., Messina, J. P., Pigott, D. M., Moyes, C. L., Hay, S. I. (2016). Predicted global distribution of Burkholderia pseudomallei and burden of melioidosis. *Nat. Microbiol Nature Microbiology, 1*(1), 15008. doi: 10.1038/nmicrobiol.2015.8.

7. West, E., Myers, N., Ligget, D., & Skerrett, S. (2012). Murine pulmonary infection and inflammation induced by inhalation of Burkholderia pseudomallei. *International Journal of Experimental Pathology, 93*, 421-428. doi: 10.1111/j.1365-2613.2012.00842.x.

8. Forouhi, N., & Wareham, N. (2014). Epidemiology of diabetes. *Medicine, 42*(12), 698–702-698–702. doi:10.1016/j.mpmed.2014.09.007.

9. Santacruz-Sanmartín, E., Hincapié-Palacio, D., Ospina, M., Perez-Toro, O., Bernal-Restrepo, L., Buitrago-Giraldo, S., Díaz, F. (2015). Seroprevalence of mumps in an epidemic period in Medellín, Colombia. *Vaccine,* 698–702. doi:10.1016/j.mpmed.2014.09.007.

10. Allwood, E., Devenish, R., Prescott, M., Adler, B., & Boyce, J. (2011). Strategies for Intracellular Survival of Burkholderia pseudomallei. *Frontiers in Microbiology, 2*, 1-19. http://dx.doi.org/10.3389/fmicb.2011.00170.

11. Sica, A., Dorman, L., Viggiano, V., Cippitelli, M., Ghosh, P., Rice, N., & Young, H. (1997). Interaction of NF- B and NFAT with the Interferon- Promoter. *Journal of Biological Chemistry, 272*(48), 30412-30420.

12. Ohmori, Y., Fukumoto, S., & Hamilton, T. (1995). Two Structurally Distinct KB Sequence Motifs Cooperatively Control LPS-Induced KC Gene Transcription in Mouse Macrophages. *The Journal of Immunology, 155*, 3593-3600.

13. Collart, M., Baeuerle, P., & Vassalli, P. (1990). Regulation of Tumor Necrosis Factor Alpha Transcription in Macrophages: Involvement of Four KB-Like Motifs and of Constitutive and Inducible Forms of NF-KB. *Molecular and Cellular Biology, 10*(4), 1498-1506.

14. Hiscott, J., Marios, J., Garoufalis, J., D'assario, M., Roulston, A., Kwan, I., Fenton, M. (1993). Characterization of a Functional NF-KdB Site in the Human Interleukin 13 Promoter: Evidence for a Positive Autoregulatory Loop. *Molecular and Cellular Biology, 13*(10), 6231-6240.

15. Cao, S. (2006). NF- B1 (p50) Homodimers Differentially Regulate Pro- and Anti-inflammatory Cytokines in Macrophages. *Journal of Biological Chemistry, 281*(36), 26041-26050. doi:10.1074/jbc.M602222200.

16. Libermann, T., & Baltimore, D. (1990). Activation of Interleukin-6 Gene Expression through the NF-KB Transcription Factor. Molecular and Cellular Biology, *10*(5), 2327-2334.

17. Tan, K. S., Chen, Y., Lim, Y. C., Tan, G. Y., Liu, Y., Lim, Y. T., Gan, Y. H. (2010). Suppression of Host Innate Immune Response by Burkholderia pseudomallei through the Virulence Factor TssM. *The Journal of Immunology, 184*(9), 5160-5171.

18. Poligone, B., & Baldwin, A. S. (2001). Positive and Negative Regulation of NF-κB by COX-2: Roles of Different Prostaglandins. *Journal of Biological Chemistry*, *276*(42), 38658-38664.

19. Hancock, R., Nijnik, A., & Philpott, D. (2012). Modulating immunity as a therapy for bacterial infections. *Nature Reviews Microbiology Nat Rev Micro, 10*, 243-254. doi:10.1038/nrmicro2745.

20. Shao, H., Lou, Z., Jeong, J., Kim, K., Lee, J., & Lee, S. (2015). Tolfenamic Acid Suppresses Inȧammatory Stimuli-Mediated Activation of NF-κB Signaling. *Biomolecules and Therapeutics Biomol Ther, 23*(1), 39-44. doi:10.4062/biomolther.2014.088.

21. Carlsen, H., Moskaug, J., Fromm, S., & Rune Blomhoff, R. (2002). In vivo imaging of NF-kappa B activity. *The Journal of Immunology, 168*(3), 1441-1446. doi:10.4049/jimmunol.168.3.1441.

22. Sadikot, R., Zeng, H., Joo, M., Everhart, M., Sherrill, T., Li, B., Blackwell, T. (2006). Targeted Immunomodulation of the NF- B Pathway in Airway Epithelium Impacts Host Defense against Pseudomonas aeruginosa. *The Journal of Immunology*, (176), 4923-4930. doi:10.4049/jimmunol.org/content/176/8/4923

23. Agard, M., Asakrah, S., & Morici, L. (2013). PGE2 suppression of innate immunity during mucosal bacterial infection. *Front. Cell. Infect. Microbiol. Frontiers in Cellular and Infection Microbiology, 3*(45). doi:10.3389/fcimb.2013.00045

24. Ricciotti, E., & FitzGerald, G. A. (2011). Prostaglandins and Inflammation. *Arteriosclerosis, Thrombosis, and Vascular Biology*, *31*(5), 986–1000. doi.org/10.1161/ATVBAHA.110.207449

25. Ralstin, M. (2006). Parthenolide Cooperates with NS398 to Inhibit Growth of Human Hepatocellular Carcinoma Cells through Effects on Apoptosis and G0-G1 Cell Cycle Arrest. *Molecular Cancer Research,* 387-399. doi:10.1158/1541-7786.MCR-05-0157.

26. Jeong, J., Yang, X., Clark, R., Choi, J., Baek, S., & Lee, S. (2013). A mechanistic study of the proapoptotic effect of tolfenamic acid: Involvement of NF- B activation. *Carcinogenesis, 34*(10), 2350-2360. doi:10.1093/carcin/bgt224

27. Sidhu, P., Landoni, M., & Lees, P. (2005). Pharmacokinetic and pharmacodynamic interactions of tolfenamic acid and marbofloxacin in goats. *Research in Veterinary Science, 80*, 79-90. doi:10.1016/j.rvsc.2005.04.008.

28. Krymchantowski, A. V., & Bigal, M. E. (2006). Rizatriptan versus rizatriptan plus rofecoxib versus rizatriptan plus tolfenamic acid in the acute treatment of migraine. *BMC Neurology*, *4*, 10. doi.org/10.1186/1471-2377-4-10.

29. Pentikalnen, P., Neuvonen, P., & Backman, C. (1981). Human pharmacokinetics of tolfenamic acid, a new anti-inflammatory agent. *European Journal of Clinical Pharmacology Eur J Clin Pharmacol*, 359-365.

30. Chowdhury, S. (2005). Oxidative Metabolites of Drug and Xenobiotics: LC-MS methods to ID and Characterize in Biological Matricies. In *Identification and Quantification of Drugs, Metabolites and Metabolizing Enzymes By LC-MS* (1st ed., Vol. 6, pp. 270-271). Amsterdam: Elsevier Science Limited.

31. Kankaanranta, H., & Moilanen, E. (1995). Flufenamic and tolfenamic acids inhibit calcium influx in human polymorphonuclear leukocytes. *Molecular Pharmacology, 47*, 1008-1013.

32. Colon, J., Basha, M., Madero-Visbal, R., Konduri, S., Baker, C., Herrera, L., Abdelrahim, M. (2009). Tolfenamic acid decreases c-Met expression through Sp proteins degradation and inhibits lung cancer cells growth and tumor formation in orthotopic mice. *Invest New Drugs Investigational New Drugs, 29*, 41-51. doi:10.1007/s10637-009-9331-8.

33. Pathi, S., Li, X., & Safe, S. (2013). Tolfenamic acid inhibits colon cancer cell and tumor growth and induces degradation of specificity protein (Sp) transcription factors. *Mol. Carcinog. Molecular Carcinogenesis, 53*(S1), E53-61. doi:10.1002/mc.22010

34. John-Aryankalayil, M., Palayoor, S., Cerna, D., Falduto, M., Magnuson, S., & Coleman, C. (2009). NS-398, ibuprofen, and cyclooxygenase-2 RNA interference produce significantly different gene expression profiles in prostate cancer cells. *Molecular Cancer Therapeutics, 8*(1), 261-273. doi:10.1158/1535-7163.MCT-08-0928.

35. Hartley, J., Evans, L., Green, K., Naghashfar, Z., Macias, A., Zerfas, P., & Ward, J. (2008). Expression of infectious murine leukemia viruses by RAW264.7 cells, a potential complication for studies with a widely used mouse macrophage cell line. *Retrovirology, 5*(1), 1-1. doi:10.1186/1742-4690-5-1.

36. Powell, K., Ulett, G., Hirst, R., & Norton, R. (2003). G-CSF immunotherapy for treatment of acute disseminated murine melioidosis. *FEMS Microbiology Letters, 224*(2), 315-318.

37. Propst, K., Mima, T., Choi, K., Dow, S., & Schweizer, H. (2010). A Burkholderia pseudomallei purM Mutant Is Avirulent in Immunocompetent and Immunodeficient Animals: Candidate Strain for Exclusion from Select-Agent Lists. *Infection and Immunity, 78*(7), 3136-3143. doi:10.1128/IAI.01313-09.

38. Saotome, K., Morita, H., & Umeda, M. (1989). Cytotoxicity test with simplified crystal violet staining method using microtitre plates and its application to injection drugs. *Toxicology in Vitro, 3*(4), 317-321. doi:10.1016/0887-2333(89)90039-8.

39. Bartholomew, J. W., & Mittwer, T. (1952). THE GRAM STAIN. *Bacteriological Reviews, 16*(1), 1–29.

40. Khursheed, M., Kolla, J., Kotapalli, V., Gupta, N., Gowrishankar, S., Uppin, S., Bashyam, M. (2013). ARID1B, a member of the human SWI/SNF chromatin remodeling complex, exhibits tumour-suppressor activities in pancreatic cancer cell lines. *Br J Cancer British Journal of Cancer, 108*, 2056-2062. doi:10.1038/bjc.2013.200

41. Castro-Garza, J., Barrios-Garcia, H., Cruz-Vega, D., Said-Fernandez, S., Carranza-Rosales, P., Molina-Torres, C., & Vera-Cabrera, L. (2007). Use of a colorimetric assay to measure differences in cytotoxicity of Mycobacterium tuberculosis strains. *Journal of Medical Microbiology, 56*, 733-737. doi:10.1099/jmm.0.46915-0.

42. Cao, H., Xiao, L., Park, G., Wang, X., Azim, A. C., Christman, J. W., & van Breemen, R. B. (2008). An improved LC-MS-MS method for the quantification of prostaglandins E_2 and D_2 production in biological fluids. *Analytical Biochemistry, 372*(1), 41–51. doi:10.1016/j.ab.2007.08.041.

43. Cummings, J., Beaupre, A., Knudson, S., Liu, N., Yu, W., Neckles, C., Slayden, R. (2013). Substituted Diphenyl Ethers as a Novel Chemotherapeutic Platform against Burkholderia pseudomallei. *Antimicrobial Agents and Chemotherapy, 58*(3), 1646-1651. doi:10.1128/AAC.02296-13

44. Miranda, B. R., Popichak, K. A., Hammond, S. L., Jorgensen, B. A., Phillips, A. T., Safe, S., & Tjalkens, R. B. (2015). The Nurr1 Activator 1,1-Bis(3'-Indolyl)-1-(p-Chlorophenyl)Methane Blocks Inflammatory Gene Expression in BV-2 Microglial Cells by Inhibiting Nuclear Factor B. *Molecular Pharmacology, 87*(6), 1021-1034.

45. Hollebeeck, S., Raas, T., Piront, N., Schneider, Y., Toussaint, O., Larondelle, Y., & During, A. (2011). Dimethyl sulfoxide (DMSO) attenuates the inflammatory response in the in vitro intestinal Caco-2 cell model. *Toxicology Letters, 206*(3), 268-275.

46. Sanmartín-Suárez, C., Soto-Otero, R., Sánchez-Sellero, I., & Méndez-Álvarez, E. (2011). Antioxidant properties of dimethyl sulfoxide and its viability as a solvent in the evaluation of neuroprotective antioxidants. *Journal of Pharmacological and Toxicological Methods, 63*(2), 209-215.

47. Pinto, L., Trivett, M., Wallace, D., Higgins, J., Baseler, M., Terabe, M., Hildesheim, A. (2005). Fixation and cryopreservation of whole blood and isolated mononuclear cells: Influence of different procedures on lymphocyte subset analysis by flow cytometry. *Cytometry Part B: Clinical Cytometry, 63B*, 47-55. doi:10.1002/cyto.b.20038.

48. Otto, O., Rosendahl, P., Mietke, A., Golfier, S., Herold, C., Klaue, D., Guck, J. (2015). Real-time deformability cytometry: On-the-fly cell mechanical phenotyping. *Nature Methods Nat Meth, 12*(3), 199-202. doi:10.1038/nmeth.3281

49. Cummings, J. E., Kingry, L. C., Rholl, D. A., Schweizer, H. P., Tonge, P. J., & Slayden, R. A. (2013). The Burkholderia pseudomallei Enoyl-Acyl Carrier Protein Reductase FabI1 Is Essential for In Vivo Growth and Is the Target of a Novel Chemotherapeutic with Efficacy. *Antimicrobial Agents and Chemotherapy, 58*(2), 931-935. doi:10.1128/AAC.00176-13.

50. Poguzhelskaya, E., Artamonov, D., Bolshakova, A., Vlasova, O., & Bezprozvanny, I. (2014). Simplified method to perform CLARITY imaging. *Molecular Neurodegeneration Mol Neurodegeneration, 9*(1), 19.

APPENDIX I

A1.1 Appendix Introduction

The purpose of this appendix is to outline a number of pilot studies conducted during this research project in effort to better characterize the cellular and animal responses to *B. pseudomallei* infection. The goal is to explain the materials and methods of these additional experiments as well as the results obtained. Ideally, these data will form a platform from which another student can continue this research in order continue to explore the effects of immune modulation during *B pseudomallei* infection.

A1.2 Material and Methods: Effect of TA on Cytokine Production

In order to character is how infection with Bp82 effects cytokine production over time, RAW 264.7 cells were used. Two million RAW 264.7 cells were plated in a three six-well plates for 24 hours. After washing, cells were infected and centrifuged for 5 minutes at 500 rpm to allow the infection to reach the monolayer.

The first experiment was a time-course in which the MOI was reduced to 1 in order to determine how cytokine production varied over 24 hours. To determine cytokine production, after each time point the cell supernatant was removed and filtered through at 0.02µm filter. The BD cytokine bead analysis kit (BD Systems) for flow cytometry was utilized in accordance with the manufactures in instructions. Samples had to be diluted by a factory in order to fall in the proper range.

After the time course results, it was found that 6 to 8 hours was ideal as cytokine production peaks during this time. Therefore, the same experiment was conducted again, only with 30 minute pre-treatments of 100µM TA, 10mg/ml Ceftazidime, and 0.01% DMSO.

A1.3 Results: Effect of TA on Cytokine Production

For the time course, it was shown that interleukin 6 (IL-6), MCP-1 and tumor necrosis factor all responded by having a time dependent increase in cytokine concentration peaking at 24 hours, where interferon gamma (IFN-γ), interleukin 10 (IL-10) and interleukin 12 (IL12p70) had peak concentrations after 8 hour and then began to decline. Therefore, any treatment-based change is visualized best after 6-8 hours after infection (Figure A1.1).

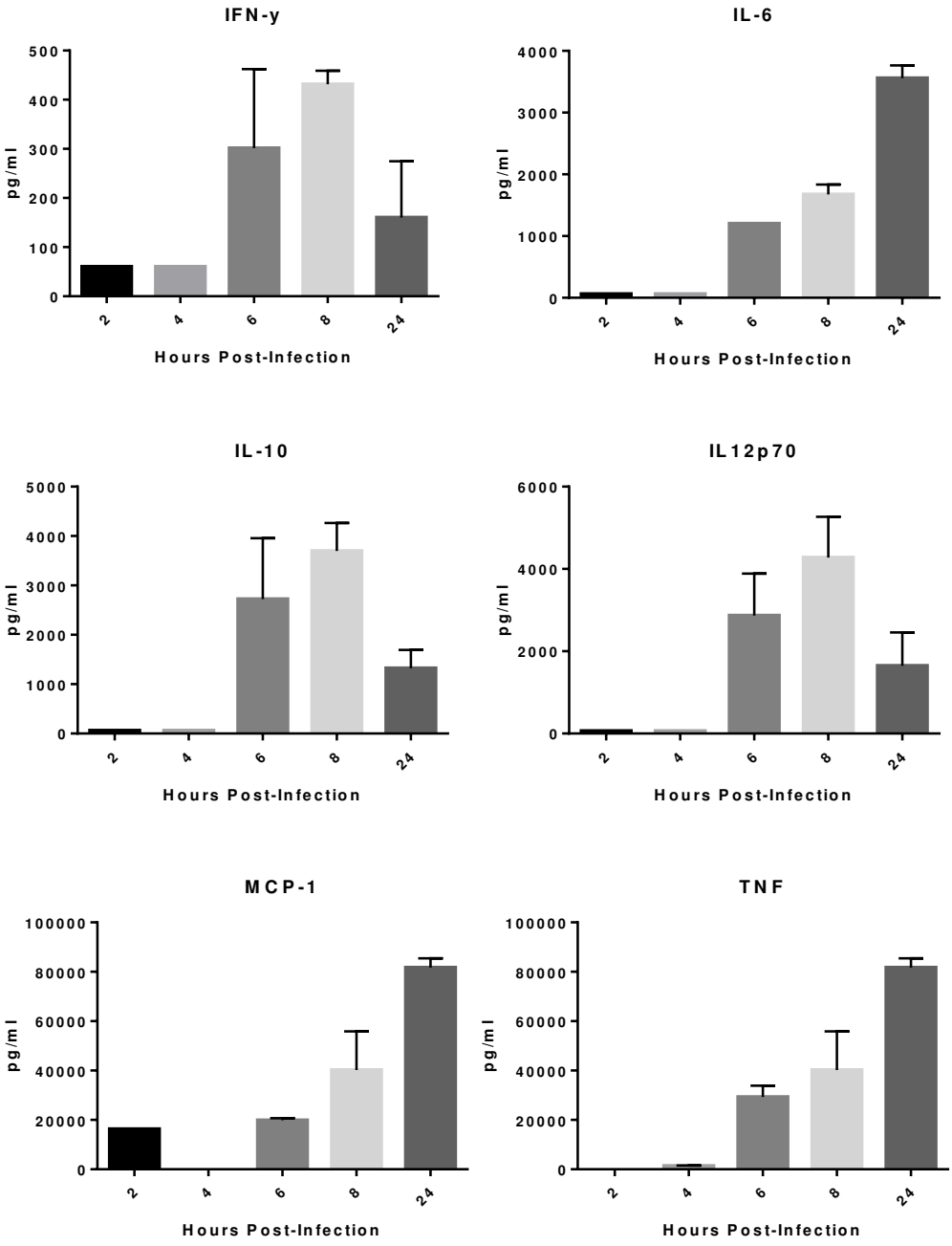

Figure A1.1. Effect of BP82 cytokine production over time. RAW 264.7 cells were infected at a MOI of 1 over 24 hours to determine how infection effects cytokine production. Half of the cytokines had a time –based increase in cytokine levels, where IFN-γ, IL-10, and IL12p70 peaked at 8 hours.

There was a treatment related change seen with treatment. Treatment with TA increased levels of IFN-γ, IL-10, IL12p70 when compared to the vehicle control, as well as all other treatment groups. TA did not seem to have an effect on MCP-1 or TNF. Treatments with Ceftazidime only reduced IL12p70.

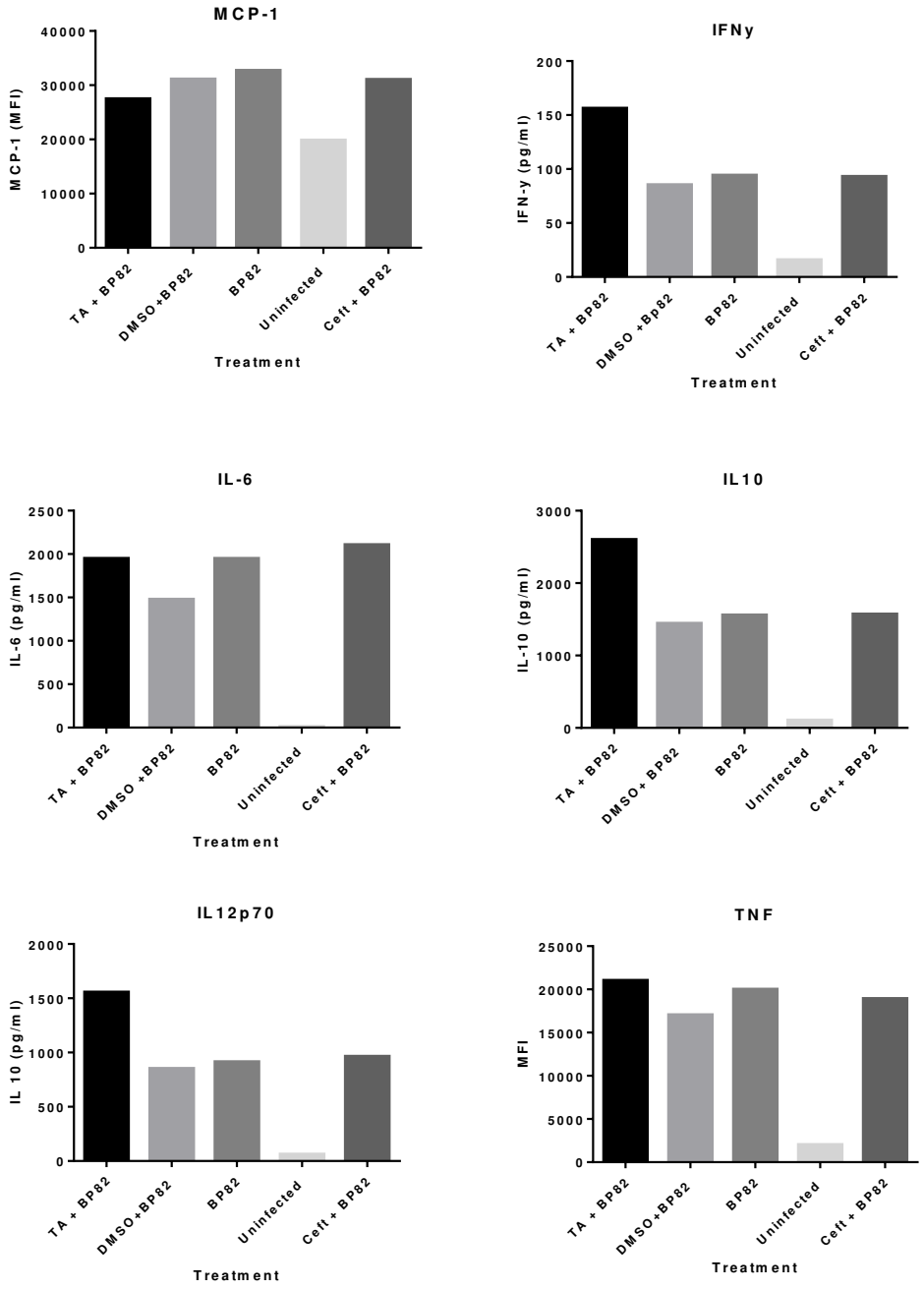

Figure A1.2. Effect of treatment on cytokine concentrations in Bp82 infected RAW. 264.7 cell after 6 hours. TA increased IL-10, IL12p70 and IL-10 levels and had little effect on other cytokines. Treatment with Ceftazidime reduced the concentration of IL12p70 only.

A1.4 Materials and Methods: Bp82 Immunofluorescence to Characterize Infection

In order to visualize the infection of RAW 264.7 cells, immunofluorescence was used. Raw 264.7 cells were plated and infected as described in section 4.17. After 6 hours of infection, cells were washed with PBS and fixed using 100% methanol for 20 minutes. Cells were blocked using 5% BSA in PBS for 30 minutes and primary anti-Burkholderia antibody (graciously provided by the Borlee Lab at Colorado State University) was added at a 1:500 dilution and allowed to stain overnight at 4°C. IF slides were washed in PBS and the secondary antibody was added in a 1:1000 dilution for 1 hour. Slides were mounted and imaged as described in 4.17.

A1.5 Results: Bp82 Immunofluorescence to Characterize Infection

The resulting images were very striking and very effective at visualizing the infection using Bp82. To my knowledge, this is the first use of this primary anti-body was used for Bp82, verifying that it is effective for Bp82 use.

A. B.

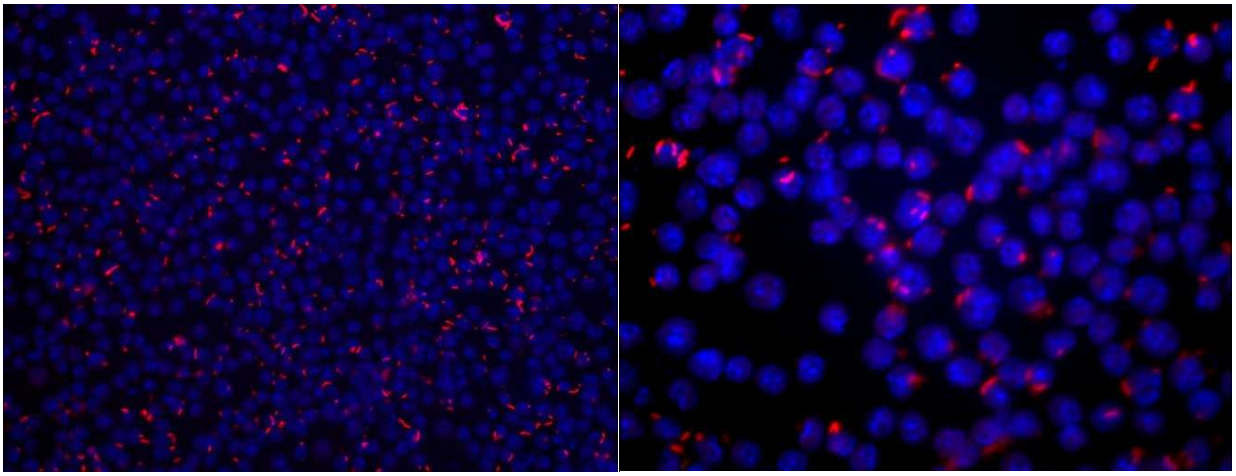

Figure A1.3. Visualization of Bp82 infection on RAW 264.7 cells. Cells were infected at an MOI of 5 for 2 hours and images at 20X (A) and 40X (B). Blue is a nuclear stain (DAPI) and red in Bp82. Because the slides were washed extensively, any Bp82 left in the image represents intracellular staining.

A1.6 Materials and Methods: CLARITY

CLARITY is in incredibly effective tool used to visualize an almost infinite number of aspects within animal organ tissue. My idea for this project was to utilize the primary antibody used in A1.5 in order to visualize the infection within the organs of the mice not used for bacterial burden counts in section 5.9.

Organ tissue from the lung liver and spleen on infected animals was fixed and stored in 10% formalin. Tissue was sliced at depths of between 100µm and 500µm and stained using the protocol outlined in [51].

A1.7 Results: CLARITY

The staining for 1026b bacteria as well as COX-2 revealed some success with the best results from the lung tissue. However, due to the difficulty of these stains, I was unable to get the clarity desired.

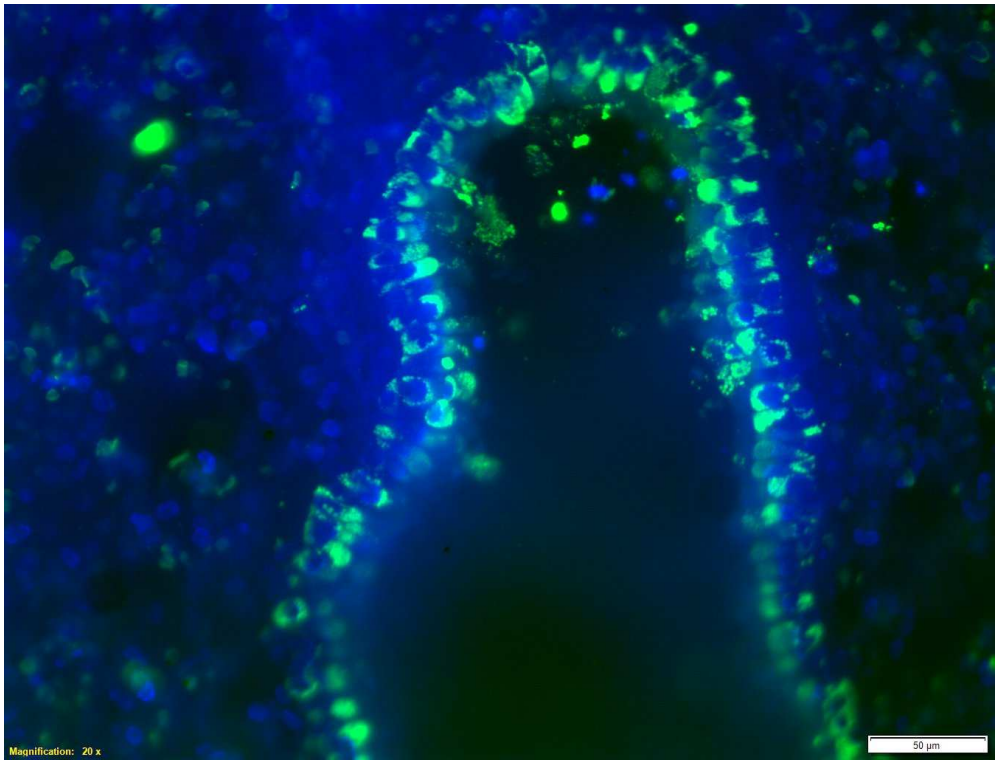

Figure A1.4 COX-2 stain in the uninfected lung of a BALB/c mouse. Tissue was stained in primary for 5 days followed for secondary anti-body for 3 days before imaging. Blue represents nuclear staining and green is a COX-2 stain.

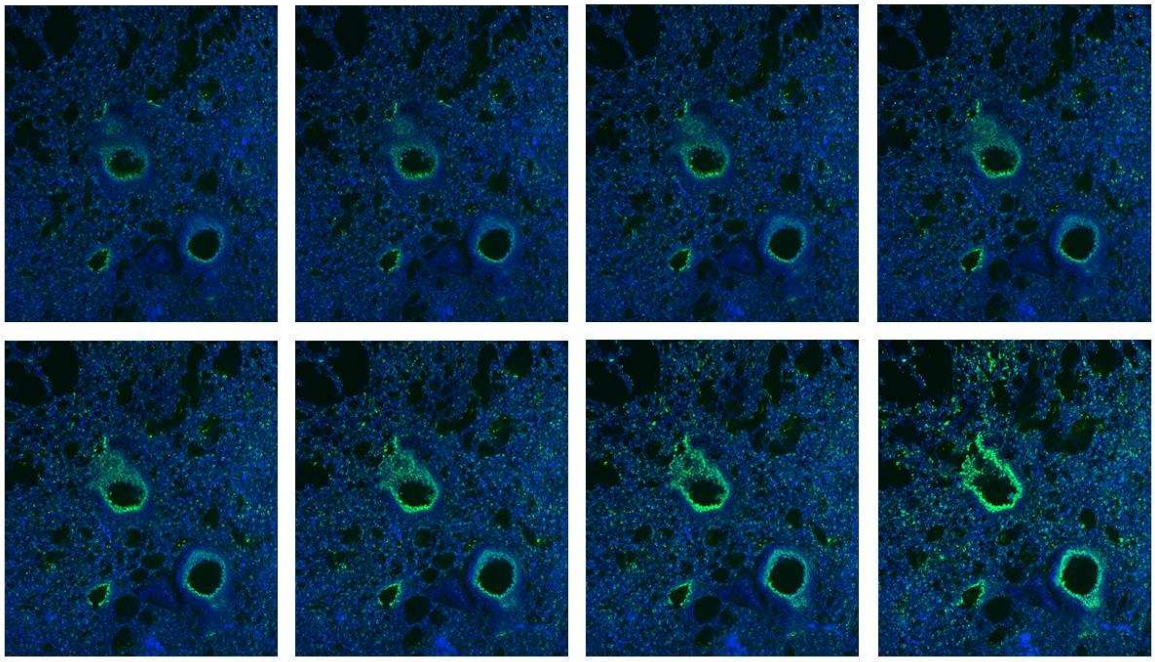

Figure A1.5. COX-2 stain in the uninfected lung of a BALB/c mouse. Tissue was stained in primary for 5 days followed for secondary anti-body for 3 days before imaging. Blue represents nuclear staining and green is a COX-2 stain. Each image is a 15 micron increase in depth one the Z axis.

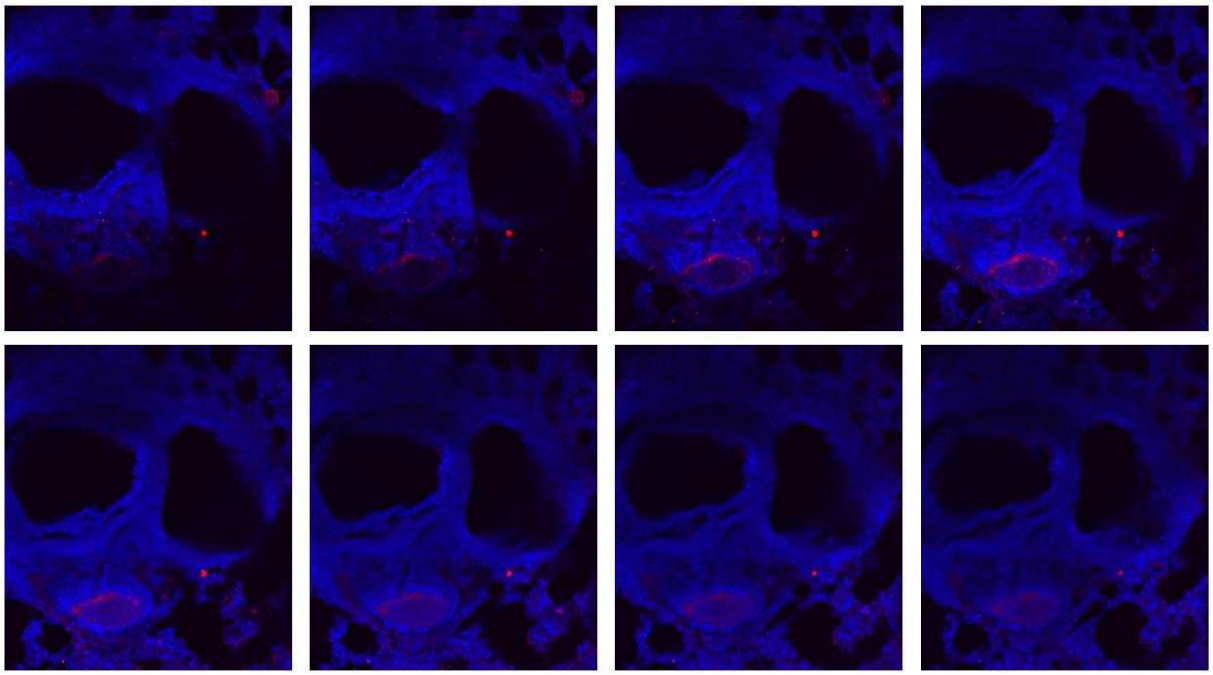

Figure A1.6. *B. pseudomallei* 1026b stain in the infected lung of a BALB/c mouse. Tissue was stained in primary for 5 days followed for secondary anti-body for 3 days before imaging. Blue represents nuclear staining and red is a 1026b stain. Each image is a 30 micron increase in depth one the Z axis.

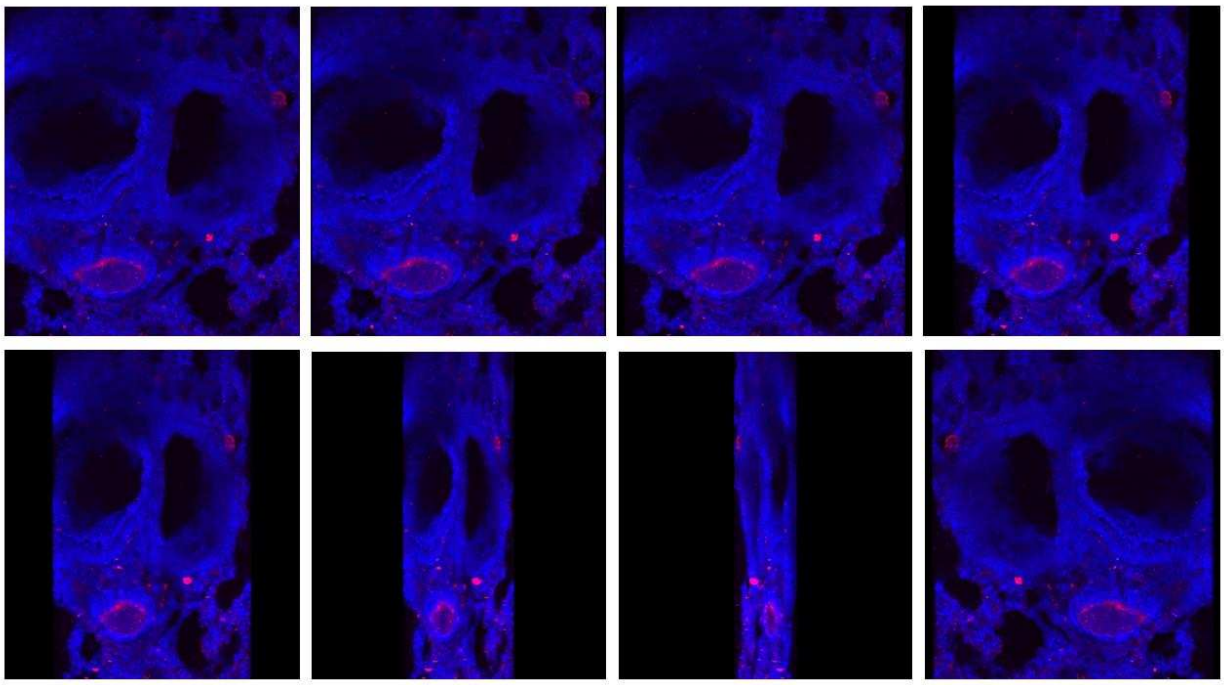

Figure A1.7. *B. pseudomallei* 1026b stain in the infected lung of a BALB/c mouse. Tissue was stained in primary for 5 days followed for secondary anti-body for 3 days before imaging. Blue represents nuclear staining and red is a 1026b stain. Image is 15 micron in depth and rotated on the Y axis clockwise with each image.

A1.8. Appendix Summary

The tools used in this appendix may be useful for anyone who would want to continue this project. First, it was revealed that treatment has a drastic change on cytokine levels of RAW 264.7 cells. This effect may be important in further elucidating the how TA is an effective treatment against Bp82. IF, and the antibodies used, are an incredible tool and should be utilized in to aid in the visualization of effective treatments. Lastly, CLARITY is an incredible, yet simple, way to visualize what is happening in the tissues. While the focus here was on inflammatory markers and the bacterial rods themselves, it would be prudent to use this method

to visualize other aspects of inflammation. For instance, characterizing the changes in inflammatory response cells within the tissue during infection may prove as a valuable experiment.